

A MATHEMATICAL MODEL OF THE PRODUCTIVITY
INDEX OF A WELL

A Dissertation

by

DINARA KHALMANOVA

Submitted to the Office of Graduate Studies of
Texas A&M University
in partial fulfillment of the requirements for the degree of

DOCTOR OF PHILOSOPHY

May 2004

Major Subject: Mathematics

A MATHEMATICAL MODEL OF THE PRODUCTIVITY
INDEX OF A WELL

A Dissertation

by

DINARA KHALMANOVA

Submitted to Texas A&M University
in partial fulfillment of the requirements
for the degree of

DOCTOR OF PHILOSOPHY

Approved as to style and content by:

Jay R. Walton
(Chair of Committee)

Thomas Blasingame
(Member)

Yalchin Efendiev
(Member)

Akif Ibragimov
(Member)

Raytcho Lazarov
(Member)

Albert Boggess
(Head of Department)

May 2004

Major Subject: Mathematics

ABSTRACT

A Mathematical Model of the Productivity

Index of a Well. (May 2004)

Dinara Khalmanova, B.S., Karaganda State University, Kazakhstan;

M.S., Texas A&M University

Chair of Advisory Committee: Dr. Jay R. Walton

Motivated by the reservoir engineering concept of the productivity index of a producing oil well in an isolated reservoir, we analyze a time dependent functional, diffusive capacity, on the solutions to initial boundary value problems for a parabolic equation. Sufficient conditions providing for time independent diffusive capacity are given for different boundary conditions. The dependence of the constant diffusive capacity on the type of the boundary condition (Dirichlet, Neumann or third-type boundary condition) is investigated using a known variational principle and confirmed numerically for various geometrical settings. An important comparison between two principal constant values of a diffusive capacity is made, leading to the establishment of criteria when the so-called pseudo-steady-state and boundary-dominated productivity indices of a well significantly differ from each other. The third type boundary condition is shown to model the thin skin effect for the constant wellbore pressure production regime for a damaged well. The questions of stabilization and uniqueness of the time independent values of the diffusive capacity are addressed. The derived formulas are used in numerical study of evaluating the productivity index of a well in a general three-dimensional reservoir for a variety of well configurations.

ACKNOWLEDGMENTS

I am grateful to Dr. Peter Valko (Department of Petroleum Engineering) for his valuable contribution to this work. I thank the referees for constructive criticism on the earlier results. Above all, I am very grateful to Dr. Jay Walton and Dr. Akif Ibragimov for their continuing professional guidance and moral support in the last four years - this work would not have been possible without their help. All errors and inconsistencies remain my own.

NOMENCLATURE

A	- symmetric positive definite matrix of smooth coefficients
C_A	- shape factor
C_Ω	- geometric characteristic of domain Ω , defined in terms of ϕ_0
h	- thickness of the reservoir
$H^{1,2}$	- Sobolev space
J	- diffusive capacity (productivity index)
L	- elliptic operator, $Lu = \nabla \cdot A\nabla u$
mes_n	- n -dimensional Lebesgue measure
q	- dimensionless rate of flow from the well
R_D	- dimensionless outer radius
s	- skin factor
V	- volume of the reservoir, $V = mes_n\Omega$
W	- surface area of the wellbore, $W = mes_{n-1}\Gamma_w$
α	- as a superscript, denotes dependence on α
Γ_w	- wellbore
Γ_e	- exterior boundary of the reservoir, $\partial\Omega = \Gamma_w \cup \Gamma_e$
ϕ_k, λ_k	- solutions of the related Sturm-Liouville problem for the operator L
∇	- gradient operator on Ω
\vec{n}	- outward normal on $\partial\Omega$
$\frac{\partial u}{\partial \vec{\nu}}$	- co-normal derivative of u on $\partial\Omega$, $\frac{\partial u}{\partial \vec{\nu}} = (A(x)\nabla u) \cdot \vec{n}$
\bar{u}_w	- average of function u on Γ_w
\bar{u}_Ω	- average of function u on Ω

TABLE OF CONTENTS

CHAPTER		Page
I	INTRODUCTION	1
	A. Layout of Dissertation	4
II	STATEMENT OF THE PROBLEM	6
	A. Definition of Diffusive Capacity	8
III	LITERATURE REVIEW	10
IV	TIME INDEPENDENT DIFFUSIVE CAPACITY	19
	A. Initial Boundary Value Problem I.	19
	B. Initial Boundary Value Problem II.	23
	C. Initial Boundary Value Problem III.	24
	D. Comparison of the Constant Diffusive Capacities for Problems I, II and III	26
V	TRANSIENT DIFFUSIVE CAPACITY	29
	A. IBVP I - Constant Production Rate Regime.	29
	B. IBVP II - Constant Wellbore Pressure Regime.	34
VI	MODEL OF THE SKIN EFFECT	39
	A. Diffusive Capacity for IBVP III in an Annulus	40
VII	PRODUCTIVITY INDEX IN A TWO-DIMENSIONAL RESER- VOIR	46
	A. Comparison to Existing Results	48
	B. Productivity Index in Non-symmetric Domains	55
	C. Productivity Index in Domains Violating Isoperimetric Inequality	56
	D. Orthotropic Media	59
VIII	PRODUCTIVITY INDEX IN A THREE-DIMENSIONAL RESERVOIR	63
	A. Directionally Drilled Wells. Effect of Vertical Flow.	69
	B. Horizontal Well	74

CHAPTER	Page
IX	REMARKS ON NUMERICAL CALCULATIONS 81
	A. Computations in Two-dimensional Domains 81
	B. Computations in Three-dimensional Domains 94
X	CONCLUSIONS AND FUTURE DIRECTIONS 97
	REFERENCES 100
	VITA 104

LIST OF TABLES

TABLE	Page
1	Productivity Indices for Typical Drainage Area Shapes. Part 1. 49
2	Productivity Indices for Typical Drainage Area Shapes. Part 2. 52
3	The Effect of the Location of the Well Relative to the Center of Gravity on the Difference Between BD and PSS PI's. 56
4	The Effect of Isoperimetric Inequality and Symmetry of the Domain on the Difference Between J_I and J_{II} 59
5	The Effect of Anisotropy on the Difference Between J_I and J_{II} 61
6	Productivity Indices for Domain D_1 , Well Configuration (B). 69
7	Productivity Indices for Domain D_2 , Well Configuration (B). 70
8	Productivity Indices for Domain D_1 , Well Configuration (A). 71
9	Productivity Indices for Domains D_2 , Well Configuration (C). 72
10	Productivity Indices for Domain D_1 , Well Configuration (C). 74
11	Productivity Indices for Domain D_1 , Well Configuration (D), Various Values of L 75
12	Productivity Indices for Domain D_1 , Well Configuration (D), Various Values of h 76
13	Effect of Grid Refinement on Computations of J_{PSS} 93
14	Effect of Grid Refinement on Computations of J_{BD} and λ_0 93
15	Order of Approximation of λ_0 94

LIST OF FIGURES

FIGURE	Page
1	Image Pattern for a Square Drainage Area with No-flow Boundaries [29]. 12
2	Schematic Representation of a Thin Skin Zone. 15
3	Radial Profile of an Initial Distribution Yielding Small Diffusive Capacity. 38
4	Graph of $s(\alpha)$ for $R_D = 1000$ 42
5	Graph of $s(\alpha)$ for $R_D = 10000$ 43
6	Graph of $J_{III}(\alpha)$ for $R_D = 1000$ 43
7	Graph of $J_{III}(\alpha)$ for $R_D = 10000$ 44
8	Eigenfunction for Negative α . $R_D = 1000$ 44
9	Eigenfunction for Positive α . $R_D = 1000$ 45
10	Domain with a Violated Isoperimetric Inequality. 58
11	Symmetrical Domain with a Violated Isoperimetric Inequality. 58
12	Schematic Representation of Domain D_1 64
13	Schematic Representation of Domain D_2 65
14	Schematic Representation of Horizontal Projection of Domain D_2 66
15	Schematic Representation of the Vertical Cross-section for Well Configuration (A). See p. 66 67
16	Schematic Representation of the Vertical Cross-section for Well Configuration (B). See p. 66 67

FIGURE	Page
17	Schematic Representation of the Vertical Cross-section for Well Configuration (C). See p. 66 67
18	Schematic Representation of the Vertical Cross-section for Well Configuration (D). See p. 66 68
19	Schematic Representation of the Vertical Cross-section for Well Configuration (E). See p. 66 68
20	Productivity Indices for Domains D_1 and D_2 for Well Configuration (B). 70
21	Productivity Indices for Domain D_1 , Well Configuration (A). 71
22	Productivity Indices for Domain D_2 , Well Configuration (C). 72
23	Productivity Indices for Domain D_1 , Well Configuration (C). 73
24	Productivity Indices for Domain D_1 , Well Configuration (D). 76
25	Pseudo-steady-state Productivity Index for Various Values of d , Well Configuration (E), $h = 500$, $L = 500$ 77
26	Pseudo-steady-state Productivity Index for Various Values of d , Well Configuration (E), $h = 500$, $L = 700$ 78
27	Pseudo-steady-state Productivity Index for Various Values of d , Well Configuration (E), $h = 500$, $L = 900$ 78
28	Pseudo-steady-state Productivity Index for Various Values of d , Well Configuration (E), $h = 500$, $L = 1100$ 79
29	Pseudo-steady-state Productivity Index for Various Values of d , Well Configuration (E), $h = 500$, $L = 1300$ 79
30	Pseudo-steady-state Productivity Index for Various Values of d , Well Configuration (E), $h = 500$, $L = 1500$ 80
31	Pseudo-steady-state Productivity Index for Various Values of d , Well Configuration (E), $h = 500$, $L = 1700$ 80

CHAPTER I

INTRODUCTION

Once the production of a hydrocarbon-bearing reservoir has started, reservoir engineers must answer three important questions. First, what is the volume of hydrocarbons present in the reservoir? Second, at what rate can the available fluid be recovered? Third, how much of the fluid can be recovered? The answers to these questions change as the reservoir develops and greatly depend on the production schemes [29, 6]. The reservoir engineer creates a picture of the reservoir/well system from the available data. Among such are the production history data, i. e. the rate of flow from the well q and the pressure on the wellbore p_w . Using the history data on the rate of flow from the well, one can readily obtain the cumulative production rate from the well. Shutting the well down and analysing the “build-up” pressure curves during the shut-in period by the methods of well test analysis [8, 29], the average pressure in the reservoir, \bar{p} , can be estimated. The productivity index of a well is a characteristic that relates these three parameters. It is defined as the ratio of the rate of flow from the well to the difference between the wellbore pressure and the average reservoir pressure [29].

The productivity index is often used as a measure of the capacity of a well [13] [29]. It expresses an intuitive feeling that, once the well production is “stabilized”, the ratio of production rate to some pressure difference between the reservoir and the well must depend on the geometry of the reservoir/well system only [29]. Indeed, it has been long ago observed by petroleum engineers that in a bounded reservoir the productivity index of a single well stabilizes in a long time asymptote [32].

The journal model is SIAM Journal on Applied Mathematics.

After the productivity index of a well has reached its stable value, the definition of the productivity index can be recast into the equation for determining the speed with which the hydrocarbon can be recovered from the reservoir:

$$q = J(\bar{p} - p_w). \quad (1.1)$$

Here, J is the stabilized value of the productivity index. Alternatively, the Fetkovich [12] backpressure equation has been used:

$$q = C(J)(\bar{p}^2 - p_w^2)^n, \quad (1.2)$$

where $C(J)$ is related to the productivity index parameter and n is an empirically determined constant.

A hydrocarbon - bearing reservoir with a single well can be produced in two substantially different regimes.

1) The pressure on the well is maintained at a constant level while the rate of flow from the well is decreasing along with the average reservoir pressure.

2) The rate of flow from the well is held constant while the wellbore pressure and the average reservoir pressure decrease.

If the productivity index of the well produced with constant wellbore pressure is constant, then the regime of recovery is called *a boundary-dominated state* [17]. The regime of recovery with the constant rate of flow from the well, characterized by a constant productivity index, is called *a pseudo-steady-state regime* [29].

From the mathematical prospective, the productivity index of a well can be defined as a functional on the solutions to an initial boundary value problem. This functional will be called *the diffusive capacity*. A constant productivity index corresponds to a time independent diffusive capacity on the transient solution to the initial boundary value problem.

The two regimes of recovery - with constant wellbore pressure and constant rate of flow from the well - are modeled by Dirichlet and Neumann boundary conditions, respectively.

When estimating the productivity index of a well, one has to take into consideration the presence of the so-called “thin-skin” zone around the well. The thin-skin concept reflects the damage occurring during drilling and completion of the well. Because of fluid invasion, the permeability of the “small” region around the well is lower than the reservoir permeability, which causes the measured pressure responses to differ from the predicted ones [33, 18]. The existence of the infinitesimally thin skin zone around the well is modeled by a third type boundary condition.

In this work we will study the properties of a constant diffusive capacity. In particular, the following questions will be addressed:

- What are the conditions providing for the constant diffusive capacity?
- How do the constant values of the diffusive capacity depend on the geometry of the boundary?
- How large can a difference between the pseudo-steady-state and boundary-dominated state productivity indices be?
- What is the relation between the diffusive capacity for different types of boundary conditions?
- How does a transitive diffusive capacity stabilize?

The derived formulas for pseudo-steady-state and boundary-dominated state productivity indices hold for an arbitrary reservoir/well geometry. A part of this dissertation is a numerical study addressing the problem of evaluation of the productivity

indices in a variety of three dimensional reservoir shapes with wells of diverse configurations, i.e., for fully or partially penetrating, and vertical or deviated wells.

A. Layout of Dissertation

Following this introduction we will formulate the initial boundary value problems governing the pressure of a fluid in a bounded reservoir with a single well and define the diffusive capacity. The Literature Review will outline the existing methods of evaluation of the productivity index of a well. In Time Independent Diffusive Capacity we give sufficient conditions for a constant diffusive capacity for each of the initial boundary value problems formulated below. In addition, analytical formulas for the constant values of the diffusive capacities will be derived. Based on the remarks given in the introduction, we will examine the correlation between three principal values of the diffusive capacity. Transient Diffusive Capacity will address the questions pertaining to the stabilization of the productivity indices in two principal regimes of production and provide several important examples on stabilization of the boundary-dominated productivity index. In Productivity Index in a Two-dimensional Reservoir the obtained formulas for the constant diffusive capacities will be applied to various shapes of a two-dimensional reservoir; it is a numerical study that will reveal several important factors influencing the magnitude of the difference between two principal constant values of productivity index. Model of the Skin Effect section is an investigation of the relation between the third and second initial boundary value problems. The Productivity Index in a Three-dimensional Reservoir section is a numerical study of the productivity indices in an isotropic homogenous bounded three-dimensional reservoir with a cylindrical well of arbitrary angle of deviation and length of penetration. A brief section, Remarks on Numerical Calculations, will com-

ment on the computing software and code used to generate the numerical results given in the previous sections. The last section will give a brief summary of the advantages of the new method of evaluation of the productivity index of a well and important properties of the diffusive capacity that were revealed in this work.

CHAPTER II

STATEMENT OF THE PROBLEM

Let a point in \mathbb{R}^n be denoted by $x = (x_1, \dots, x_n)$, $n = 2, 3$. Let Ω be an open domain in \mathbb{R}^n which is bounded by the two disjoint piecewise smooth surfaces Γ_w and Γ_e . Let $u(x, t)$, $t \in \mathbb{R}$, be a solution of the equation

$$\frac{\partial u}{\partial t} = Lu, \quad (2.1)$$

where $L = \nabla \cdot (A(x)\nabla)$, A is a symmetric positive definite matrix with smooth components and $\nabla = (\frac{\partial}{\partial x_1}, \dots, \frac{\partial}{\partial x_n})$ is the usual gradient operator.

Let $u(x, t)$ be subject to homogeneous Neumann boundary condition on Γ_e :

$$\frac{\partial u}{\partial \vec{\nu}} = (A(x)\nabla u) \cdot \vec{n} = 0, \quad (2.2)$$

where \vec{n} is the outward normal to Γ_e . On the remaining part of the boundary, Γ_w , three types of boundary conditions will be considered:

- a) constant total flux $\int_{\Gamma_w} \frac{\partial u}{\partial \vec{\nu}} dS = -q$, q being a real positive constant;
- b) constant Dirichlet condition $u|_{\Gamma_w} = u_{w2}$, u_{w2} - real positive constant;
- c) mixed boundary condition $((u - u_{w3})|_{\Gamma_w} + \alpha \frac{\partial u}{\partial \vec{\nu}})|_{\Gamma_w} = 0$, where α and u_{w3} are real constants.

This leads to three initial boundary value problems:

Problem I:

$$Lu = \frac{\partial u}{\partial t}, \quad x \in \Omega, \quad t > 0$$

$$\frac{\partial u}{\partial \vec{\nu}}|_{\Gamma_e} = 0,$$

$$\int_{\Gamma_w} \frac{\partial u}{\partial \nu} dS = -q,$$

$$u(x, 0) = f_1(x).$$

Problem II:

$$Lu = \frac{\partial u}{\partial t}, \quad x \in \Omega, \quad t > 0$$

$$\frac{\partial u}{\partial \nu} |_{\Gamma_e} = 0,$$

$$u|_{\Gamma_w} = u_{w2},$$

$$u(x, 0) = f_2(x).$$

Problem III:

$$Lu = \frac{\partial u}{\partial t}, \quad x \in \Omega, \quad t > 0$$

$$\frac{\partial u}{\partial \nu} |_{\Gamma_e} = 0,$$

$$(\alpha \frac{\partial u}{\partial \nu} + (u - u_{w3}))|_{\Gamma_w} = 0,$$

$$u(x, 0) = f_3(x).$$

For simplicity, we assume that the components of the coefficient matrix A and the domain boundary are smooth, so solutions of the problems I, II and III are understood in a classical sense. In problem II, $u_{w2} > 0$ is a given constant; in problem III, $u_{w3} > 0$ is the average of u on Γ_w and α is a given constant.

Several remarks regarding the sign of the solutions of problems I, II and III are in order. Physically $u(x, t)$ is interpreted as the fluid pressure in the reservoir, hence, we will restrict our attention only to positive solutions of problems I, II and III.

Note that problem I is not well posed: if a solution exists, then there is an infinite number of solutions. Moreover, a solution to problem I is not necessarily positive on Ω for all $t > 0$, even if the initial function $f_1(x)$ is positive on Ω . It will be shown that

for positive q , there exists a solution to problem I which is positive on Ω for $t \in (0, T)$ for some positive T .

The maximum principle for a parabolic equation implies that the solution of problem II is unique and positive if the initial condition f_2 is positive on Ω [10]. The uniqueness, existence and regularity of the solutions of problem III with respect to the sign of the coefficient α in the boundary condition on Γ_w are discussed, for example, in [14].

A. Definition of Diffusive Capacity

Let us introduce the following notation. If v is a function defined on Ω , then let \bar{v}_w and \bar{v}_Ω denote the average of v on Γ_w and Ω , respectively, defined by:

$$\bar{v}_w = \frac{1}{W} \int_{\Gamma_w} v dS,$$

and

$$\bar{v}_\Omega = \frac{1}{V} \int_{\Omega} v dx,$$

where $V = \text{mes}_n \Omega$, $W = \text{mes}_{n-1} \Gamma_w$.

Definition 1. Let $u(x, t)$ be a classical solution [14] of the parabolic equation $Lu = \frac{\partial u}{\partial t}$ in $\Omega \times (0, \infty)$ with boundary condition $\frac{\partial u}{\partial \bar{\nu}}|_{\Gamma_e} = 0$ and either a), b) or c) on Γ_w . Let $T > 0$ be such that $u(x, t) > 0$ for all $x \in \Omega$ and $t \in (0, T)$. The Diffusive Capacity of Γ_w with respect to Γ_e (or simply Diffusive Capacity) for the solution $u(x, t)$ is the ratio:

$$J(u, t) = \frac{\int_{\Gamma_w} \frac{\partial u}{\partial \bar{\nu}} dS}{\bar{u}_w - \bar{u}_\Omega}, \quad (2.3)$$

where $t \in (0, T)$.

In our intended application, Ω represents a hydrocarbon reservoir with a flowing fluid (oil) with the outer boundary Γ_e and a well with boundary Γ_w . The outer

boundary of the reservoir is assumed impermeable to the flowing fluid. It is assumed that the fluid is slightly compressible and its flow in the reservoir is governed by Darcy's Law relating the gradient of pressure in the reservoir to the filtration velocity [27, 29]. Then $u(x, t)$ corresponds to the pressure in the reservoir and the three types of boundary conditions specified on the well Γ_w correspond to different recovery regimes. Boundary condition (a) models the recovery regime with constant production rate, boundary condition (b) models the recovery regime with constant wellbore pressure, and (c) models the constant well bore pressure regime of production from a well with nonzero skin [29]. The initial conditions f_1 , f_2 and f_3 take on a meaning of the pressure distribution in the reservoir Ω , hence, we will require that $f_i \geq 0$ on Ω , $i = 1, 2, 3$. The IBVP III will be discussed in greater detail in the section Model of Skin Effect. The diffusive capacity $J(u, t)$ takes on the meaning of the productivity index of the well.

CHAPTER III

LITERATURE REVIEW

The evaluation of the productivity index of a well is based on the analysis of a well test. A well test is a record of variations of the wellbore pressure with time, when the well rate is controlled in some specific manner. One of the popular well tests is a shut-in test, where the well is kept closed (zero rate), allowing the wellbore pressure to increase. The variation of the wellbore pressure in this case is called a build-up curve [29]. After the well tests are completed, the build-up curves are analyzed and interpreted to yield the estimates of the important reservoir characteristics, for example, permeability, average reservoir pressure, productivity index, etc [8, 29, 9]. Here the most relevant methods and techniques of the well test analysis for evaluation of the productivity index will be discussed[30].

In 1949, van Everdingen and Hurst presented solutions for the problem of single-phase fluid influx into a cylindrical reservoir of uniform thickness h , permeability k and porosity ϕ . In their work [33], the fluid is assumed to have a small constant compressibility c , viscosity μ and the flow is governed by Darcy's law. Ignoring gravity effects and using axisymmetry in cylindrical geometry, the pressure $p(r, t)$ in the reservoir satisfies the diffusivity equation

$$\frac{\partial^2 p}{\partial r^2} + \frac{1}{r} \frac{\partial p}{\partial r} = \frac{\phi \mu c}{k} \frac{\partial p}{\partial t}. \quad (3.1)$$

They nondimensionalize the problem by means of the following transformation, which then became customary to reservoir engineering:

$$p_D(r_D, t_D) = \frac{2\pi k h (p_i - p)}{q \mu}, \quad (3.2)$$

$$r_D = \frac{r}{r_w}, \quad (3.3)$$

$$t_D = \frac{kt}{\phi\mu cr_w^2}, \quad (3.4)$$

where r_w is the wellbore radius, q is the rate of flow from the well and p_i is the uniform initial pressure distribution in the reservoir. van Everdingen and Hurst considered the case of a constant production rate q and applied the Laplace transform to compute the dimensionless pressure drop for a unit value of r_D .

When infinite systems are considered, the wellbore radius is negligibly small and the boundary condition on the wellbore becomes [29]:

$$\lim_{r \rightarrow r_w} \left(r \frac{\partial p}{\partial r} \right) = \frac{q}{2\pi kh}. \quad (3.5)$$

The solution to this problem was provided by Theis in 1935 [31] and is usually referred to by his name:

$$p_D(r_D, t_D) = -\frac{1}{2} Ei\left(-\frac{r_D^2}{4t_D}\right), \quad (3.6)$$

where $-Ei(-x) = \int_x^\infty \frac{e^{-s}}{s} ds$ for $x > 0$. When the argument of the exponential integral Ei is small enough, i. e. when $r_D^2/4t_D < 0.01$, it can be closely approximated by

$$p_D(r_D, t_D) \approx -\frac{1}{2} \left(\ln \frac{r_D^2}{4t_D} + 0.5772 \right). \quad (3.7)$$

Matthews, Brons and Hasebroek in [24] applied the method of superposition of the solutions (3.6) and (3.7) to derive the solution to the problem of flow in a bounded reservoir of appropriate geometric shape. This method is usually referred to as the method of images, which can be summarized as follows.

Assume that two wells are produced with the same rate. Then on the line located on equal distance from both wells, there is no flux - normal derivative of pressure is equal to zero. Thus, this line corresponds to a sealing fault or no-flow boundary. This idea can be easily extended to a square drainage area with a well located in the center of the square. The image pattern for such a reservoir is represented on Fig.1.

Each of the wells represented by solid circles is produced with the same rate as the well located in the center of the square drainage area with boundaries represented by thick lines on Fig. 1. For this square drainage area, the flux of pressure on the boundaries is zero.

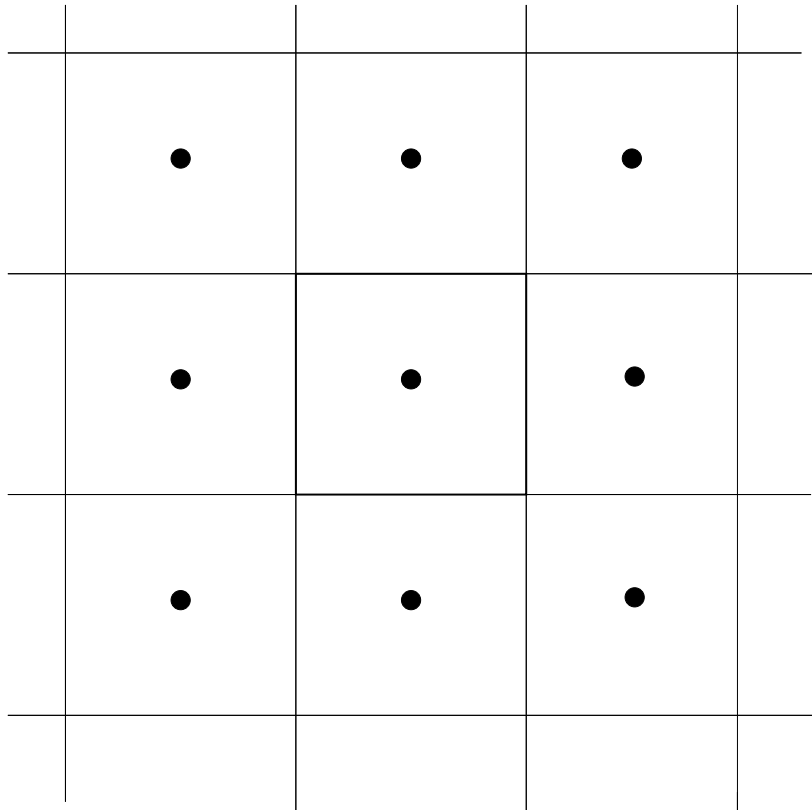


Fig. 1. Image Pattern for a Square Drainage Area with No-flow Boundaries [29].

Following this example, the method of images can be applied to other shapes of a bounded drainage area. A bounded drainage area of a polygonal shape with a single well with impermeable boundaries is translated infinitely many times in all directions to cover the entire 2-D plane. These translated wells resulting from such construction are called image wells. The real well in the original bounded drainage area is not necessarily located in the center of the drainage area. The pressure $p_D(x_D, y_D, t_D)$ inside the original bounded drainage area is equivalent to superposition of infinitely

many solutions to the problem with a single well in an infinite reservoir, each of which is determined by (3.6) or (3.7). The superposition in [24] has been written as:

$$p_D(x_D, y_D, t_{DA}) = \sum_{i=1}^{\infty} p_D(a_{iD}, t_{DA}), \quad (3.8)$$

where $a_{iD} = a_i/\sqrt{A}$, a_i - distance from the i th image well to the point (x_D, y_D) , x_D and y_D are any convenient dimensionless coordinates, A - drainage area of the bounded system and

$$t_{DA} = \frac{kt}{\phi\mu cA}. \quad (3.9)$$

The dimensionless time t_{DA} , introduced in [24], is useful in determining the average pressure in the reservoir \bar{p} from the material balance equation (neglecting wellbore storage):

$$\frac{kh}{\mu} \frac{p_i - \bar{p}}{q} = t_{DA}. \quad (3.10)$$

Another useful feature of this particular nondimensionalization of time is that it can be defined for any 2-D drainage area, not only a circular one. In their work, Matthews, Brons and Hazebroek presented results for a variety of drainage shapes to which the method of images can be applied.

In 1965, Dietz has presented a modified method of evaluating the average reservoir pressure for a single well produced with constant rate from a bounded reservoir[7]. He assumed that the system has reached its pseudo-steady-state, when the rate of change of pressure is uniformly constant throughout the reservoir. In pseudo-steady-state, the dimensionless wellbore pressure is given by [29],[17]

$$p_{wD}(t_{DA}) \approx 2\pi t_{DA} + \frac{1}{2} \ln \left(\frac{4A}{e^{\gamma} C_A r_w^2} \right) + s, \quad (3.11)$$

where s is a skin factor. The concept of the skin factor and methods of its assessment are discussed below. In Eq.(3.11), C_A is called the *shape factor*. It depends on the

geometry of the drainage area. In his work [7] Dietz computed the shape factors C_A for a variety of drainage shapes using the results of Matthews, Brons and Hasebroek. Eq.(3.11) and the material balance equation (3.10) can be combined to obtain a formula for approximate dimensionless pseudo-steady-state productivity index of a well:

$$PI_D \approx \frac{1}{\frac{1}{2} \ln \frac{4A}{e^\gamma C_A r_w^2} + s}. \quad (3.12)$$

In contrast to the constant rate production scheme, not much attention has been paid to a boundary-dominated productivity index. In fact, it is a belief in the reservoir engineering community that the boundary-dominated state productivity index and pseudo-steady-state productivity index do not differ significantly for most drainage area shapes.

In 1998, Wattenbarger and Helmy considered the constant wellbore pressure production case [17]. They applied a method of superposition to generate a solution to the corresponding boundary value problem in a bounded reservoir and used an important correlation between the transforms of the cumulative production and the variable rate of production in Laplace space to derive shape factors in (3.12) for the boundary-dominated productivity index. They showed that productivity indices computed with the new shape factors can differ by as much as 10% from the productivity index with Dietz's shape factors even for simple drainage shapes. In the numerical study on the productivity indices in two dimensional drainage areas given in section Productivity Index in a Two-dimensional Reservoir the results presented in [7] and [17] will be compared to the results obtained with the formulas presented in this dissertation.

The concept of skin effect was introduced by van Everdingen [34] and Hurst [18] in 1953. They suggested that the difference between the measured and predicted pressure on the wellbore, observed by many authors before them, is due to the dam-

aged zone around the wellbore. Almost every field operation - drilling, completion, production - causes damage to the zone adjacent to the wellbore. As a result, the permeability in this so-called *skin zone* is lower than in the formation causing an additional pressure drop in the skin zone during flow toward the well [21]. Disregarding the skin effect leads to overestimation of the productivity index of a well.

The concept introduced by van Everdingen and Hurst corresponds to the so-called *thin skin*, when the difference between the radius of the skin zone r_s and the wellbore radius r_w is negligibly small (see Fig.2). van Everdingen, in [34], denoted the dimensionless pressure drop Δp_D within the skin zone by *s - skin factor*. The thin skin s appears in the approximate formula for the productivity index (3.12). Positive skin corresponds to a damaged well.

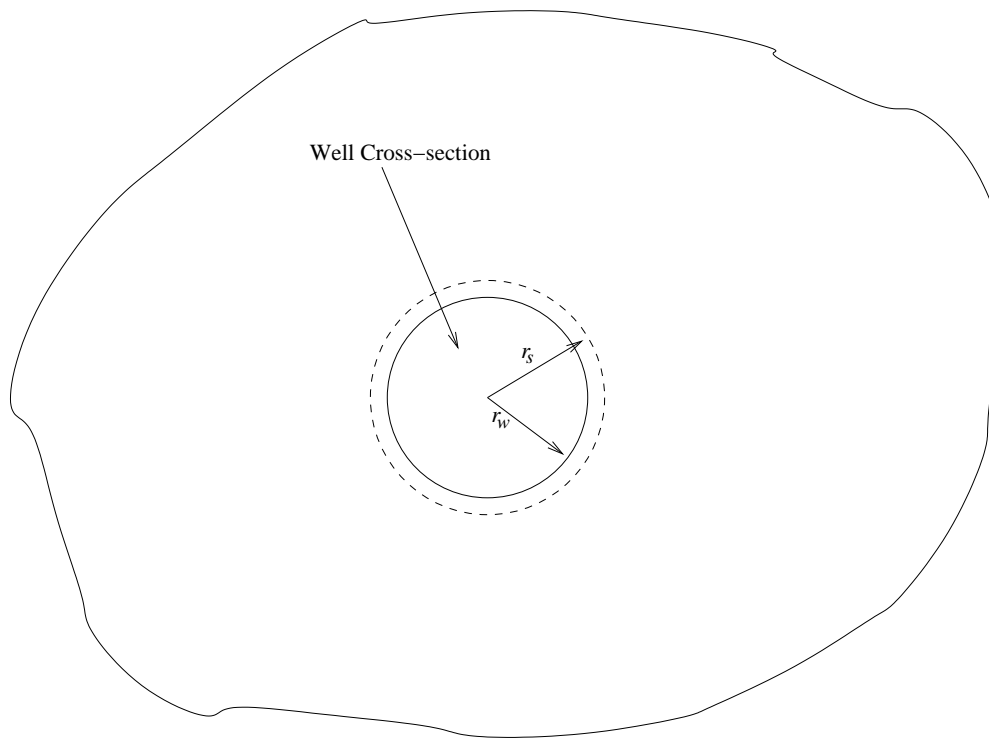


Fig. 2. Schematic Representation of a Thin Skin Zone.

One of the unappealing features of the thin-skin concept is the assumption that

the thickness of the skin zone is negligibly small. Hawkins [16] assumed that the skin zone has a finite thickness, i. e. $|r_s - r_w|$ is not infinitesimal and derived the following formula, often referred to by his name:

$$s = \left(\frac{k}{k_s} - 1 \right) \ln \frac{r_s}{r_w}, \quad (3.13)$$

where k_s is the permeability of the skin zone and it is assumed that the flow through the skin zone is at steady-state.

In [16] it was also shown that under the assumption of the finite thickness of the skin zone and steady-state flow in it, s cannot be less than -6 , negative skin s corresponding to a stimulated well. Later in 1969, Hurst et al. showed that if the wellbore radius is assumed to be greater than the skin zone radius, the same equations as for positive skin can be applied to describe the pressure on the wellbore for a stimulated well with negative skin[19]. It should be noted that despite the fact that extensive research on the skin effect has been carried out for the constant rate production regime, little attention has been paid to the constant pressure production regime.

The majority of solutions for evaluating the productivity index in three-dimensional reservoirs, i. e. for directionally drilled wells, follow the same principle as the two-dimensional methods. In that they are based on a semi-analytical solution for a particular case, from which one finds a convenient approximate formula which is then applied to similar reservoir/well configurations. The semi-analytical solution is often based on the superposition of analytical solutions for a transient problem in an unbounded reservoir. The solution in a bounded reservoir is then expressed in terms of an infinite time dependent series, similarly to the technique used by Matthews, Brons and Hazebroek in [24]. Then a comprehensive computing procedure is applied to determine the stabilized values of the time dependent series in the obtained

solution [22, 28, 35].

In most cases the methods for computing the productivity index of a deviated or horizontal well in a three dimensional reservoir are aimed at obtaining an appropriate value of a shape factor C_A and skin factor s in the Eq. (3.12). The effects associated with the deviation of the well from a fully penetrated vertical one are included in the skin s . A vertical well is called fully penetrated if its penetration length is equal to the thickness of the reservoir. A vertical fully penetrated well corresponds to $s = 0$. The effects of the geometry of the external boundaries of the reservoir are included in the shape factor C_A [22]. Here we will discuss several representative works on evaluation of the productivity index in a three dimensional reservoir.

Goode and Kuchuk [15] have considered a horizontal well in a rectangular reservoir bounded from above and below. They restricted the thickness of the reservoir to be small in comparison to the distance of the well to any of the vertical boundaries of the reservoir. Then the problem can be viewed as a two dimensional with the horizontal well treated as a two dimensional plane source. The two dimensional problem is solved by using the Laplace transform and the value of the productivity index is evaluated numerically. The neglected effects of the vertical flow are included in the geometric skin, s_g . The authors provided results for a range of well length values [15]. The boundary condition on the well is an “infinite conductivity” condition, i.e., the pressure is uniformly distributed over the wellbore surface. Other authors used similar technique of reducing the three dimensional problem to a two dimensional one treating a well as a vertical fracture with uniform flux rather than uniform pressure distribution over the length of wellbore (see [22], for example).

Cinco et al. considered a directionally drilled well in a cylindrical reservoir bounded from above and below [4, 3]. They used the solution for a problem with a point source well in an infinite three dimensional reservoir and integrated it along

the well under the assumption that the flux is uniform along the wellbore surface. The obtained result can be superimposed by the method of images to yield the desired solution in cylindrical coordinate system. The authors presented results for various penetration lengths and angles of deviation[3].

A similar technique can be applied to reservoirs with shapes other than cylindrical as was done in [22]. Larsen has presented results for two basic drainage shapes - cylindrical and rectangular and for various deviation angles and penetration lengths.

As seen from this review, the existing methods and techniques of evaluation of the productivity index impose serious restrictions on the geometry of the reservoir. In particular, the vertical dimension of the reservoir has to be small in comparison to its lateral dimensions to allow one to neglect the flow in the vertical direction or include its effect in the geometrical skin, s_g . Another restriction is due to the use of the method of images, which requires the drainage area shape to be convex and suitable for covering the whole plane when translated infinitely many times.

One should also note that very little attention has been paid to methods for evaluating a boundary-dominated productivity index. For instance, all papers mentioned above are concerned only with evaluating the pseudo-steady-state productivity index in three-dimensional reservoir. In practice, the boundary-value productivity index values are taken to be equal to the pseudo-steady-state productivity index, despite the fact that Wattenbarger and Helmy have shown that the difference between these two values of productivity index can be up to 10% even for horizontal flow in simple drainage shapes [17].

CHAPTER IV

TIME INDEPENDENT DIFFUSIVE CAPACITY

In this chapter we show that for each of the initial boundary value problems (I, II and III) there exist initial distributions $f_1(x)$, $f_2(x)$ and $f_3(x)$, respectively, such that the diffusive capacity with respect to the corresponding problem is constant [20]. In addition, the class of solutions to the initial boundary value problem I will be described on which the diffusive capacity takes a unique constant value. In the last section the time independent values of the diffusive capacity for problems I, II and III are compared to each other.

A. Initial Boundary Value Problem I.

Remark. If $u(x, t)$ is a solution of problem I and $J(u, t) = J(u)$ is constant for all $t > 0$, then there exist real constants C and B such that

$$\bar{u}_w = \frac{1}{W} \int_{\Gamma_w} u dS = C + Bt. \quad (4.1)$$

This can be seen from the following argument. From the definition of the diffusive capacity (2.3) it follows that $\bar{u}_w = -\frac{q}{J(u)} + \bar{u}_\Omega$. Hence, $\frac{\partial \bar{u}_w}{\partial t} = \frac{\partial \bar{u}_\Omega}{\partial t}$. The divergence theorem implies that

$$\frac{\partial \bar{u}_\Omega}{\partial t} = \frac{1}{V} \int_{\Omega} L u dx = \frac{1}{V} \int_{\Gamma_w} \frac{\partial u}{\partial \bar{\nu}} dS. \quad (4.2)$$

Consequently, $\frac{\partial \bar{u}_w}{\partial t} = -\frac{q}{V}$, from which (4.1) easily follows.

Let $u_1(x)$ be the solution to the auxiliary steady-state problem:

$$L u_1 = -\frac{1}{V} \quad (4.3)$$

$$u_1|_{\Gamma_w} = 0 \quad (4.4)$$

$$\frac{\partial u_1}{\partial \vec{\nu}}|_{\Gamma_e} = 0. \quad (4.5)$$

Let the initial condition in problem (I) be $f_1(x) = qu_1(x)$. Then there exists a solution $u(x, t)$ such that the diffusive capacity is constant and is equal to:

$$J(u) = \frac{V}{\int_{\Omega} u_1(x) dx}. \quad (4.6)$$

To show that this is true, let $u(x, t) = qu_1(x) - \frac{q}{V}t$. By virtue of the divergence theorem,

$$\int_{\Gamma_w} \frac{\partial u}{\partial \vec{\nu}} dS = -q.$$

Consequently, u is a solution of the initial boundary value problem I with the initial distribution $f_1(x) = qu_1(x)$.

The diffusive capacity $J(u, t)$ on $u(x, t)$ is constant and is equal to

$$J_I := J(u, t) = \frac{V}{\int_{\Omega} u_1(x) dx}. \quad (4.7)$$

Function u is positive on Ω only for $t \in (0, T)$, where

$$T = \frac{\min_{x \in \Omega} u_1(x)}{V}. \quad (4.8)$$

Solutions of problem I represent the pressure distribution in the reservoir at time t , hence, we are interested in the positive on Ω solutions only. Therefore, the diffusive capacity (as a model of a pseudo-steady-state productivity index) $J(u, t) = J_I$ is defined only for $t \in (0, T)$, where T is given by (4.8).

Note that at each time t , $u(x, t)$ is constant on Γ_w . Consider a class of solutions to problem I that have a similar property, i. e., let class of solutions to problem I $\mathcal{U} = \{ u \mid \exists C \text{ and } B - \text{constants, such that } u(x, t) = C + Bt \text{ for } x \in \Gamma_w \text{ and for } t > 0 \}$. Let solution u of problem I with the initial condition $f_1 = qu_1$ on Ω be such that

$u \in \mathcal{Y}$. We will show that $J(u, t) = J(u)$ is equal to J_I .

To this end, we need to show the uniqueness of the solution of problem I in class \mathcal{Y} . Assume that $u \in \mathcal{Y}$ and $w \in \mathcal{Y}$ are solutions of problem I. Let C_1, B_1, C_2 and B_2 are such that for $t > 0$,

$$u(x, t)|_{\Gamma_w} = C_1 + B_1 t$$

and

$$v(x, t)|_{\Gamma_w} = C_2 + B_2 t.$$

Then the difference $g(x, t) = u(x, t) - v(x, t)$ is the solution of the following initial boundary value problem:

$$Lg = \frac{\partial g}{\partial t}, \quad x \in \Omega, \quad t > 0, \quad (4.9)$$

$$\frac{\partial g}{\partial \vec{\nu}}|_{\Gamma_e} = 0, \quad (4.10)$$

$$g|_{\Gamma_w} = (C_1 - C_2) + (B_1 - B_2)t, \quad (4.11)$$

$$g(x, 0) = 0. \quad (4.12)$$

Trivial initial condition (4.12) immediately implies $C_1 = C_2$.

Consider function $h = \frac{\partial g}{\partial t}$. It is a solution of the following problem:

$$Lh = \frac{\partial h}{\partial t}, \quad x \in \Omega, \quad t > 0, \quad (4.13)$$

$$\frac{\partial h}{\partial \vec{\nu}}|_{\Gamma_e} = 0, \quad (4.14)$$

$$h|_{\Gamma_w} = B_1 - B_2, \quad (4.15)$$

$$h(x, 0) = 0. \quad (4.16)$$

In addition, from the boundary condition on Γ_w of problem I and the divergence

theorem it follows that for $t > 0$

$$\begin{aligned} \int_{\Omega} h dx &= \frac{\partial}{\partial t} \int_{\Omega} g dx = \int_{\Omega} Lg dx = \int_{\Gamma_w} \frac{\partial g}{\partial \vec{\nu}} \\ &= \int_{\Gamma_w} \frac{\partial g}{\partial \vec{\nu}} - \int_{\Gamma_w} \frac{\partial g}{\partial \vec{\nu}} = 0. \end{aligned} \quad (4.17)$$

Without loss of generality, assume that $B_1 > B_2$. From the maximum principle for parabolic equation and the trivial initial condition (4.16) it follows that $h(x, t) \geq 0$ $\forall x \in \Omega$ and $t > 0$. As a solution of the parabolic equation (4.13) with the constant Dirichlet condition (4.15) on one part of the boundary $\partial\Omega$ and trivial Neumann condition (4.14) on the remaining part of $\partial\Omega$, h will converge to a constant $B_1 - B_2$ on Ω as $t \rightarrow \infty$. Together with condition (4.17) this implies that

$$(B_1 - B_2)V = \lim_{t \rightarrow \infty} \int_{\Omega} h(x, t) dx = 0. \quad (4.18)$$

Thus, $u = v$. Consequently, we have proved the following

Proposition 1. *If both conditions (i) and (ii) are satisfied:*

(i) *solution $u(x, t)$ of problem I is in class $\Upsilon = \{ u \mid \exists C \text{ and } B - \text{constants, such that } u(x, t) = C + Bt \text{ for } x \in \Gamma_w \text{ and for } t > 0 \}$;*

(ii) *the initial condition in problem I is given by $f_1(x) = qu_1(x)$, where u_1 is a solution of problem (4.3)-(4.5),*

then the diffusive capacity on the solution u of problem I is constant and is given by

$$J(u, t) = J_I = \frac{V}{\int_{\Omega} u_1 dx}.$$

From the proof preceding Proposition 1 it also follows that problem I has a unique solution in class Υ . The condition imposed on u in proposition 1 corresponds to the infinite conductivity condition on the wellbore, i. e., the conductivity of the wellbore is assumed to be so great with respect to the velocity filtration of fluid

into the wellbore, that the pressure of the incoming fluid in the wellbore equalizes instantly. From proposition 1 it follows that if the wellbore is assumed to have an infinite conductivity and the initial distribution is qu_1 then the productivity index for a well produced with constant rate is constant and is given by J_I .

B. Initial Boundary Value Problem II.

Let

$$\frac{\partial u_2}{\partial t} = Lu_2, \quad (4.19)$$

$$\frac{\partial u_2}{\partial \vec{\nu}}|_{\Gamma_e} = 0, \quad (4.20)$$

$$u_2|_{\Gamma_w} = 0, \quad (4.21)$$

$$u_2(x, 0) = f_2(x) - u_{w2}. \quad (4.22)$$

Obviously, $u(x, t) = u_2(x, t) + u_{w2}$ solves problem II. Then the diffusive capacity for problem II can be expressed in terms of $u_2(x, t)$, namely

$$J(u, t) := J(u_2, t) = \frac{\int_{\Gamma_w} \frac{\partial u_2}{\partial \vec{\nu}} dS}{-\frac{1}{V} \int_{\Omega} u_2(x, t) dx} \quad (4.23)$$

Consider the related Sturm-Liouville problem for the elliptic operator L and the first eigenpair of the latter, i.e, let λ_0 and $\phi_0(x)$ be the first eigenvalue and first eigenfunction, respectively, of the problem

$$L\phi_0 = -\lambda_0\phi_0, \quad (4.24)$$

$$\phi_0|_{\Gamma_w} = 0 \quad (4.25)$$

$$\frac{\partial \phi_0}{\partial \vec{\nu}}|_{\Gamma_e} = 0. \quad (4.26)$$

Let $u_2(x, t)$ be a solution of the initial boundary value problem (4.19)- (4.22) with the initial distribution $u_2(x, 0)$ equal to $\phi_0(x)$. Then $u_2(x, t) = \phi_0(x)e^{-\lambda_0 t}$ is a solution of

the initial boundary value problem (4.19)-(4.22). The diffusive capacity is constant and is equal to

$$J_{II} := J(u_2, t) = \frac{\lambda_0 \int_{\Omega} \phi_0(x) dx e^{-\lambda_0 t}}{\frac{1}{V} \int_{\Omega} \phi_0(x) dx e^{\lambda_0 t}} = \lambda_0 V. \quad (4.27)$$

This leads to

Proposition 2. *If the initial condition of problem II is given by $f_2(x) = \phi_0(x) + u_{w2}$, where ϕ_0 is the eigenfunction of problem (4.24)-(4.26) corresponding to the minimal eigenvalue λ_0 , then the diffusive capacity on the solution u of problem II is constant and is given by*

$$J(u, t) = J_{II} = \lambda_0 V.$$

In fact, the diffusive capacity is constant provided that the initial distribution $u_2(x, 0)$ is equal to any eigenfunction $\phi_i(x)$, $i = 1, 2, \dots$. However, only the eigenfunction corresponding to the minimal eigenvalue does not change sign on Ω , therefore, in terms of the pressure distribution in the hydrocarbon reservoir, $\phi_0(x)$ is the only physically realistic initial distribution.

C. Initial Boundary Value Problem III.

Let $u_3(x, t) = u(x, t) - u_{w3}$ where u_3 solves (III). Then $u_3(x, t)$ is a solution of the reduced problem

$$Lu_3 = \frac{\partial u_3}{\partial t}, \quad (4.28)$$

$$\frac{\partial u_3}{\partial \vec{\nu}}|_{\Gamma_e} = 0, \quad (4.29)$$

$$\left(\alpha \frac{\partial u_3}{\partial \vec{\nu}} + u_3\right)|_{\Gamma_w} = 0, \quad (4.30)$$

$$u_3(x, 0) = f_3(x) - u_{w3}, \quad (4.31)$$

Diffusive capacity $J(u, t)$ corresponding to problem (III) is expressed in terms of

$J(u_3, t)$ in the following way

$$J(u, t) = J(u_3, t) = \frac{\int_{\Gamma_w} \frac{\partial u_3}{\partial \vec{\nu}} dS}{-\frac{1}{V} \int_{\Omega} u dx}, \quad (4.32)$$

where and $\bar{u}_3|_{\Gamma_w} = 0$ is the average of u_3 on Γ_w .

Physically, the Neumann boundary condition on Γ_w in problem III corresponds to production from a well with a thin-skin zone with constant wellbore pressure (constant $\bar{u}_3|_{\Gamma_w}$) [29]. A sufficient condition for the diffusive capacity to be constant is similar to that for the second initial boundary value problem.

In particular, consider the related Sturm-Liouville problem. Let λ_k^α and $\phi_k^\alpha(x)$ be an eigenpair of the problem

$$L\phi_k^\alpha = -\lambda_k^\alpha \phi_k^\alpha, \quad (4.33)$$

$$\frac{\partial \phi_k^\alpha}{\partial \vec{\nu}}|_{\Gamma_e} = 0. \quad (4.34)$$

$$\phi_k^\alpha + \alpha \frac{\partial \phi_k^\alpha}{\partial \vec{\nu}}|_{\Gamma_w} = 0 \quad (4.35)$$

Here, the superscript α is intended to emphasize that the solution and, hence, the diffusive capacity, of problem III depend on the value of parameter α . This dependence will be analyzed in subsequent sections. Let $u_3(x, t)$ be a solution of the initial boundary value problem (4.28)- (4.31) with the initial distribution $u_3(x, 0) = \phi_k^\alpha(x)$. Then $u_3(x, t) = \phi_k^\alpha(x)e^{-\lambda_k^\alpha t}$ solves (4.28)-(4.31) and the diffusive capacity is time independent.

When parameter α in problem III is positive, then the minimal eigenvalue λ_0^α is positive and the corresponding eigenfunction $\phi_0^\alpha(x)$ does not change sign on Ω .

In chapter Model of the Skin Effect we will show that the boundary condition on Γ_w of problem III models skin effect for a damaged well produced with a constant wellbore pressure. As it is mentioned in Literature Review, the production from a

stimulated well is modeled by a negative skin factor s , therefore, we will analyze the behavior of the diffusive capacity on the solutions of problem III for negative values of parameter α . The latter case will be discussed in more detail in chapter Model of the Skin Effect. For the purposes of this chapter, it is sufficient to note that when $\alpha < 0$, the minimal eigenvalue and hence the constant diffusive capacity may be negative. Negative productivity index is an indication of injection into the well, therefore, to avoid the contradiction, our attention will be restricted to positive eigenvalues only. The analysis of the first eigenfunction will be given in chapter Model of the Skin Effect.

Regardless of the sign of α , let λ_0^α be the first nonnegative eigenvalue. If the initial distribution in (4.28)-(4.31) is equal to the corresponding eigenfunction, the constant diffusive capacity is given by

$$J_{III}(\alpha) := J(u_3, t) = \lambda_0^\alpha V, \quad (4.36)$$

Therefore, we have shown the following

Proposition 3. *If the initial condition of problem III is given by $f_3(x) = \phi_0^\alpha(x) + u_{w3}$, where ϕ_0^α is the eigenfunction of problem (4.33)-(4.35) corresponding to the minimal positive eigenvalue λ_0^α , then the diffusive capacity on the solution u of problem III is constant and is given by*

$$J(u, t) = J_{III}(\alpha) = \lambda_0^\alpha V.$$

D. Comparison of the Constant Diffusive Capacities for Problems I, II and III

The steady-state auxiliary problem (4.3)-(4.5) that was introduced before has a convenient variational formulation, which facilitates deriving an important relation between the time independent diffusive capacities of Γ_w with respect to Γ_e in Ω .

Assume that the initial distributions in problems I, II and III are such that the diffusive capacities for the problem I, II and III (J_I , J_{II} and $J_{III}(\alpha)$, respectively) - are time independent and their values are given by (4.7), (4.27) and (4.36).

Let $H^{1,2}(\Omega)$ be the usual Sobolev space [1]. Denote by $\overset{\circ}{H}{}^{1,2}(\Omega, \Gamma_w)$ the closure in $H^{1,2}(\Omega)$ norm of smooth functions that vanish on Γ_w , and by $\overset{\circ}{H}{}^{1,2}(\Omega, \Gamma_w, \alpha)$ the closure in $H^{1,2}(\Omega)$ norm of smooth functions such that $(u + \alpha \frac{\partial u}{\partial \nu})|_{\Gamma_w} = 0$ [1].

The following are well known variational principles yielding the first eigenvalues λ_0 and λ_0^α of the problems (4.24)-(4.26) and (4.33)-(4.35), respectively (see [26, 5]):

$$\lambda_0 = \inf_{u \in \overset{\circ}{H}{}^1(\Omega, \Gamma_e)} \frac{\int_{\Omega} A \nabla u \cdot \nabla u dx}{\int_{\Omega} u^2 dx}, \quad (4.37)$$

$$\lambda_0^\alpha = \inf_{u \in \overset{\circ}{H}{}^1_2(\Omega, \Gamma_w, \alpha)} \frac{\int_{\Omega} A \nabla u \cdot \nabla u dx + \frac{1}{\alpha} \int_{\Gamma_w} u^2 dS}{\int_{\Omega} u^2 dx}. \quad (4.38)$$

These two principles imply that for any positive α_1 and α_2 such that (see [5]) $\alpha_1 > \alpha_2$, $\lambda_0^{\alpha_1} < \lambda_0^{\alpha_2}$. Moreover, $\lambda_0^\alpha \nearrow \lambda_0$ as $\alpha \searrow 0$. This leads to

Proposition 4. *If the initial conditions in problems II and III are such that J_{II} and $J_{III}(\alpha)$ are time independent and $\alpha \searrow 0$, then $J_{III}(\alpha) \nearrow J_{II}$.*

Another important comparison can be made between the time independent capacities for problems I and II.

Theorem 1. *If the initial conditions in problems I and II are such that the diffusive capacities J_I and J_{II} are time independent, then*

$$J_{II} \leq J_I \leq C_{\Omega} J_{II}, \quad (4.39)$$

where $C_{\Omega} = \frac{\max_{\Omega} \phi_0}{\phi_0}$.

Proof. Let $u_1 \in \overset{\circ}{H}{}^1_2(\Omega, \Gamma_w)$ be a solution of the problem (4.3)-(4.5). We need to show

that

$$\frac{1}{\int_{\Omega} u_1(x) dx} \geq \lambda_0.$$

From (4.37) it follows that

$$\lambda_0 \leq \frac{\int_{\Omega} (\nabla u_1) \cdot (A \nabla u_1) dx}{\int_{\Omega} u_1^2 dx}. \quad (4.40)$$

Using the identity:

$$\nabla \cdot (A \nabla u_1) = (\nabla u_1) \cdot (A \nabla u_1) - u_1 \nabla \cdot (A \nabla u_1),$$

applying the divergence theorem to the numerator and making use of (4.3)- (4.5), we obtain:

$$\lambda_0 \leq \frac{1}{V} \frac{\int_{\Omega} u_1 dx}{\int_{\Omega} u_1^2 dx}. \quad (4.41)$$

The last inequality can be rewritten as

$$\lambda_0 \leq \frac{1}{V} \frac{(\int_{\Omega} u_1 dx)^2}{\int_{\Omega} u_1^2 dx} \frac{1}{\int_{\Omega} u_1 dx} \quad (4.42)$$

The first part of (4.39) now follows from Hölder's inequality.

Let $u_1(x)$ be a solution of (4.3)-(4.5) and ϕ_0 - of (4.24)-(4.26). After multiplication of both sides of (4.3) by ϕ_0 , using symmetry of A in the identity

$$(\nabla \cdot (A \nabla u_1)) \phi_0 = \nabla \cdot (\phi_0 A \nabla u_1) - \nabla \cdot (u_1 A \nabla \phi_0) + \nabla \cdot (A \nabla \phi_0) u_1, \quad (4.43)$$

followed by integration over Ω , from the divergence theorem one concludes that

$$\lambda_0 \max_{\Omega} \phi_0 \int_{\Omega} u_1 dV \geq \lambda_0 \int_{\Omega} u_1 \phi_0 dV = \frac{1}{V} \int_{\Omega} \phi_0 dV = \bar{\phi}_0. \quad (4.44)$$

The latter can be recast as the second part of (4.39), using the positivity of u_1 and ϕ_0 . □

CHAPTER V

TRANSIENT DIFFUSIVE CAPACITY

In chapter Time Independent Diffusive Capacity it was shown that the productivity index of a well in a reservoir is constant for all $t > 0$ provided that the pressure distribution at $t = 0$ satisfies certain conditions. The productivity index is known to stabilize in a long time asymptote regardless of the initial pressure distribution. In this chapter we will consider a transient diffusive capacity and investigate questions related to its stabilization. Thus, we will analyze problem I and problem II with arbitrary initial conditions. The only restriction that is imposed on the initial conditions f_1 and f_2 of problems I and II, respectively, is motivated by physical considerations: we require f_1 and f_2 be positive smooth functions on Ω .

A. IBVP I - Constant Production Rate Regime.

In Literature Review it was mentioned that the constant rate regime is usually modeled with one of two assumptions: at each time $t > 0$ either the pressure or the pressure flux is assumed to be constant on the wellbore. Proposition 1 of the previous chapter shows that the condition of the constant wellbore pressure at each time $t > 0$ (infinite conductivity condition) is equivalent to the conditions of the pseudo steady-state, i. e., the productivity index of a well is time independent. In this section we will show that the class \mathcal{Y} of solutions of problem I, defined in chapter Time Independent Diffusive Capacity, is stable with respect to small perturbations of boundary conditions. Recall that \mathcal{Y} is the class of solutions u of problem I such that at each time $t > 0$ u is constant on Γ_w . Then the stability of \mathcal{Y} is established by the following two propositions.

Proposition 5. *Let $u(x, t)$ be a solution of problem I such that $u(x, t) = Bt + h(x, t)$ for $x \in \Gamma_w$, where function $h(x, t)$ - a smooth bounded function. $\forall \epsilon > 0 \exists \delta > 0$, a constant $C > 0$ and a solution of problem I $\tilde{u} \in \mathcal{Y}$ such that if $\forall t > 0$, $|h(x, t) - C| \leq \delta \forall x \in \Gamma_w$ then $|J(u, t) - J(\tilde{u}, t)| \leq \epsilon \forall t > 0$.*

Proof. Function h is bounded on Γ_w . Let $C = \frac{1}{2}(\max_{\Gamma_w} u + \min_{\Gamma_w} u)$ and let $M = \max_{\Gamma_w} |h(x, t) - C|$. Let \tilde{u} be a solution of problem I such that $\tilde{u}|_{\Gamma_w} = C + Bt$ and $\tilde{u}(x, 0) = u(x, 0)$. Then function $v(x, t) = u(x, t) - \tilde{u}(x, t)$ is a solution of the following problem:

$$Lv = \frac{\partial v}{\partial t}, \quad x \in \Omega, \quad t > 0, \quad (5.1)$$

$$\frac{\partial v}{\partial \bar{\nu}}|_{\Gamma_e} = 0, \quad (5.2)$$

$$v|_{\Gamma_w} = h(x, t) - C, \quad (5.3)$$

$$v(x, 0) = 0. \quad (5.4)$$

The maximum principle for parabolic equation (5.1) implies that $|v(x, t)| \leq M$ for all $x \in \Omega$ and $t \geq 0$. In addition, by proposition 1, the diffusive capacity on \tilde{u} is uniquely defined.

Since $\int_{\Gamma_w} \frac{\partial u}{\partial \bar{\nu}} dS = \int_{\Gamma_w} \frac{\partial \tilde{u}}{\partial \bar{\nu}} dS = -q$ for $t \geq t_0$,

$$\left| \frac{1}{J(\tilde{u}, t)} - \frac{1}{J(u, t)} \right| \leq \frac{1}{q} \left| \frac{1}{W} \int_{\Gamma_w} (u - \tilde{u}) dS + \frac{1}{V} \int_{\Omega} (u - \tilde{u}) dx \right|.$$

Hence, $\left| \frac{1}{J(\tilde{u}, t)} - \frac{1}{J(u, t)} \right| \leq \frac{1}{q} M \left(\frac{1}{W} + \frac{1}{V} \right)$. □

In the introductory chapter it was mentioned that two principal regimes of production (constant rate of flow or constant wellbore pressure production) are idealizations of the real conditions. Certainly, the rate of flow from the well is not time independent, however, it is reasonable to assume that it is sufficiently close to a constant. Assume that this is the case. In addition, assume that at each time $t > 0$ the

wellbore pressure distribution is almost constant. That is, let $v(x, t)$ be a solution of the following initial boundary value problem:

$$Lv = \frac{\partial v}{\partial t}, \quad x \in \Omega, \quad t > 0 \quad (5.5)$$

$$\frac{\partial v}{\partial \bar{\nu}}|_{\Gamma_e} = 0, \quad (5.6)$$

$$\int_{\Gamma_w} \frac{\partial v}{\partial \bar{\nu}} dS = -q + \delta(x, t), \quad (5.7)$$

$$v(x, 0) = v_0(x). \quad (5.8)$$

Let $\delta(x, t)$ be a bounded smooth function and $\delta > 0$ be such that $\delta(x, t) < \delta \forall x \in \Gamma_w$ and $\forall t > 0$. In addition, assume that $\delta_1 > 0$ and real constants C and B are such that

$$v(x, t)|_{\Gamma_w} = C + Bt + h(x, t), \text{ where } |h(x, t)| \leq \delta_1 \quad \forall x \in \Omega, \quad \forall t > 0. \quad (5.9)$$

Along with problem(5.5)-(5.8), consider function \tilde{u} which solves problem I with the initial condition v_0 , i. e.

$$L\tilde{v} = \frac{\partial \tilde{v}}{\partial t}, \quad x \in \Omega, \quad t > 0 \quad (5.10)$$

$$\frac{\partial \tilde{v}}{\partial \bar{\nu}}|_{\Gamma_e} = 0, \quad (5.11)$$

$$\int_{\Gamma_w} \frac{\partial \tilde{v}}{\partial \bar{\nu}} dS = -q, \quad (5.12)$$

$$\tilde{v}(x, 0) = v_0(x). \quad (5.13)$$

Dirichlet-to-Neumann map for the parabolic equation (5.5) is bounded, function v is subject to condition (5.9), hence, there exists function $\tilde{h}(x, t)$ defined on Γ_w and $\delta_2 > 0$ such that the solution of the problem (5.10)-(5.13) satisfies the condition:

$$\tilde{v}(x, t)|_{\Gamma_w} = C + Bt + \tilde{h}(x, t), \text{ where } |\tilde{h}(x, t)| \leq \delta_2 \quad \forall x \in \Gamma_w, \quad \forall t > 0.$$

Let $\epsilon > 0$, then, by proposition 5, we can choose δ and δ_1 so that if g is a solution of

of problem I with $f_1 = v_0$ on Ω such that $g(x, t) = C + Bt \forall x \in \Gamma_w$ and $\forall t > 0$ then $|J(\tilde{v}, t) - J(g, t)| < \epsilon/2$. In addition, from the boundary condition (5.7) and condition (5.9) it follows that δ and δ_1 can be chosen so that $|J(\tilde{v}, t) - J(v, t)| \leq \epsilon/2$. Thus, we have proved the following.

Proposition 6. $\forall \epsilon > 0 \exists \delta > 0$ and $\delta_1 > 0$ such that if v is a solution of problem (5.5)-(5.8), the condition (5.9) holds and g is a solution of of problem I with $f_1 = v_0$ on Ω such that $g(x, t) = C + Bt \forall x \in \Gamma_w$ and $\forall t > 0$ then $|J(v, t) - J(g, t)| \leq \epsilon \forall t > 0$.

One should note that J_I is shown to be the unique value of the pseudo-steady-state productivity index of a well only under the assumption of the infinite conductivity of the well. The extent to which such assumption is realistic for various reservoir/well configurations will be discussed in more detail in chapter Productivity Index in a Three-dimensional Reservoir. Below we will investigate the question of the uniqueness of the value of the pseudo-steady-state productivity index. Recall that the pseudo-steady-state productivity index is a constant value of the diffusive capacity on the solutions to problem I. Therefore, we should consider other classes of solutions of the problem I. Then it is not hard to show the following

Remark. J_I is not necessarily a unique constant value of the diffusive capacity on the solutions to problem I.

Consider solutions to problem I with a constant flux on Γ_w , i. e. let $u(x, t)$ be a solution of the following problem

$$Lu = \frac{\partial u}{\partial t}, \quad x \in \Omega, \quad t > 0, \quad (5.14)$$

$$\frac{\partial u}{\partial \vec{\nu}}|_{\Gamma_e} = 0, \quad (5.15)$$

$$\frac{\partial u}{\partial \vec{\nu}}|_{\Gamma_w} = -\frac{q}{W}, \quad (5.16)$$

$$u(x, 0) = f_1(x). \quad (5.17)$$

The solution to (5.14)-(5.17) is given (up to an additive constant) by $u(x, t) = qv - \frac{q}{V}t + h(x, t)$, where $v(x)$ is a solution of the steady state problem

$$Lv = -\frac{1}{V}, \quad x \in \Omega, \quad (5.18)$$

$$\frac{\partial u}{\partial \vec{\nu}}|_{\Gamma_e} = 0, \quad (5.19)$$

$$\frac{\partial u}{\partial \vec{\nu}}|_{\Gamma_w} = -\frac{1}{W}, \quad (5.20)$$

and $h(x, t)$ is a solution of the corresponding problem with homogeneous boundary conditions:

$$Lh = \frac{\partial h}{\partial t}, \quad x \in \Omega, \quad t > 0, \quad (5.21)$$

$$\frac{\partial h}{\partial \vec{\nu}}|_{\Gamma_e} = 0, \quad (5.22)$$

$$\frac{\partial h}{\partial \vec{\nu}}|_{\Gamma_w} = 0, \quad (5.23)$$

$$h(x, 0) = f_1(x) - qv(x). \quad (5.24)$$

The solution to (5.21)-(5.24) is given by $h(x, t) = \sum_{n=0}^{\infty} c_n \phi_n(x) e^{-\lambda_n t}$, where $\phi_n(x)$ and λ_n are solutions of the related Sturm-Liouville problem and c_n are the coefficients of the Fourier expansion of $h(x, 0)$ in terms of ϕ_n . The diffusive capacity $J(u, t)$ is given by

$$J(u, t) = \frac{-q}{\bar{v}_w - \bar{v}_\Omega + \bar{h}_w - \bar{h}_\Omega}, \quad (5.25)$$

Note that \bar{v}_w and \bar{v}_Ω are constant, while \bar{h}_w and \bar{h}_Ω are functions of time. Clearly, the difference $\bar{h}_w - \bar{h}_\Omega = \sum_{n=0}^{\infty} c_n (\bar{\phi}_{nw} - \bar{\phi}_{n\Omega}) e^{-\lambda_n t}$ converges to a constant as $t \rightarrow \infty$, therefore, $J(u, t)$ converges to a constant value \hat{J} as $t \rightarrow \infty$. However, \hat{J} is not necessarily equal to J_I .

B. IBVP II - Constant Wellbore Pressure Regime.

For simplicity, consider the following problem for a parabolic equation. Let $u(x, t)$ be a solution of:

$$Lu = \frac{\partial u}{\partial t}, \quad x \in \Omega, \quad t \geq 0, \quad (5.26)$$

$$\frac{\partial u}{\partial \vec{\nu}}|_{\Gamma_e} = 0, \quad (5.27)$$

$$u|_{\Gamma_w} = 0, \quad (5.28)$$

$$u(x, 0) = u_0(x), \quad (5.29)$$

where $u_0(x) > 0$. Then the diffusive capacity is simply

$$J(u, t) = V \frac{\int_{\Gamma_w} \frac{\partial u}{\partial \vec{\nu}} dS}{\int_{\Omega} u dx}, \quad (5.30)$$

Effectively, problem I was “shifted down” by u_{w2} - the Dirichlet boundary condition on Γ_w . Therefore, the positivity of u_0 is equivalent to the requirement that the value of pressure set on the wellbore is less than the pressure everywhere else in the reservoir - a perfectly reasonable assumption for real production conditions.

Along with (5.26)-(5.29), consider related Sturm-Liouville problem for the operator L ,

$$L\phi_k = -\lambda_k \phi_k, \quad x \in \Omega, \quad t \geq 0, \quad (5.31)$$

$$\frac{\partial \phi_k}{\partial \vec{\nu}}|_{\Gamma_e} = 0. \quad (5.32)$$

$$\phi_k|_{\Gamma_w} = 0. \quad (5.33)$$

Let $\{\phi_k(x)\}_{k=0}^{\infty}$ be an orthonormal family of solutions of (5.31)- (5.33) with respect to the usual inner product in $L^2(\Omega)$.

Denote $d_k = \int_{\Omega} \phi_k(x) dx$ and $c_k = \int_{\Omega} u_0(x) \phi_k(x) dx$. Then the diffusive capacity

can be written as

$$J(u, t) = V \frac{\sum_{k=0}^{\infty} c_k \lambda_k d_k e^{-\lambda_k t}}{\sum_{k=0}^{\infty} c_k d_k e^{-\lambda_k t}}.$$

The last expression can be rewritten as

$$J(u, t) = V \frac{c_0 d_0 \lambda_0 e^{-\lambda_0 t} \left(1 + \sum_{k=1}^{\infty} \frac{c_k d_k \lambda_k}{c_0 d_0 \lambda_0} e^{-(\lambda_k - \lambda_0)t} \right)}{c_0 d_0 e^{-\lambda_0 t} \left(1 + \sum_{k=1}^{\infty} \frac{c_k d_k}{c_0 d_0} e^{-(\lambda_k - \lambda_0)t} \right)}.$$

At last, the latter can be recast into

$$J(u, t) = V \lambda_0 \left[1 + \frac{\sum_{k=1}^{\infty} \frac{c_k d_k}{c_0 d_0} \left(\frac{\lambda_k}{\lambda_0} - 1 \right) e^{-(\lambda_k - \lambda_0)t}}{1 + \sum_{k=1}^{\infty} \frac{c_k d_k}{c_0 d_0} e^{-(\lambda_k - \lambda_0)t}} \right]. \quad (5.34)$$

Since $\lambda_0 < \lambda_1 < \lambda_3 < \dots$, as $t \rightarrow \infty$, $J(u, t) \rightarrow \lambda_0 V$. This proves the following

Proposition 7. *If u is a solution of initial boundary value problem II, then the diffusive capacity $J(u, t)$ converges to constant value J_{II} as $t \rightarrow \infty$ for any initial condition f_2 .*

In terms of the productivity index, proposition 7 can be rephrased in the following way: if a well is produced with a constant wellbore pressure, the productivity index stabilizes to constant value J_{II} as $t \rightarrow \infty$ regardless of the initial pressure distribution.

Note that since the initial condition $u_0(x)$ is positive on Ω , $c_0 > 0$ and $d_0 > 0$. From the maximum principle for parabolic equation (5.26) it follows that $u(x, t) \geq 0$ for all $t > 0$. Consequently, the denominator in (5.34), equal to $\int_{\Omega} u(x, t) dx / c_0 d_0 e^{-\lambda_0 t}$, is positive for all $t > 0$. Therefore, from (5.34) follows

Remark. If in (5.34) $c_k d_k > 0 \forall k$, then $J(u, t) \searrow \lambda_0 V$.

The last observation allows one to analyze several physically important examples of the transient productivity index in terms of the diffusive capacity on the solutions of the initial boundary value problem for a parabolic equation.

Example 1. Suppose that a well is produced with constant rate and the productivity index is constant and the well has infinite conductivity. Then the pressure in the reservoir $u(x, t)$ is determined (up to an additive constant) by $u(x, t) = qu_1(x) - \frac{q}{V}t$ (see proposition 1), where $u_1(x)$ is a solution of the auxiliary steady-state problem

$$Lu_1(x) = -\frac{1}{V}, \quad x \in \Omega$$

$$\frac{\partial u_1}{\partial \vec{\nu}}|_{\Gamma_e} = 0,$$

$$u_1|_{\Gamma_w} = 0.$$

Suppose that at some time $t_0 > 0$, the production regime was changed to a constant wellbore pressure production. Then the pressure in the reservoir $u(x, t)$ for $t > t_0$ is defined by $u(x, t) = v(x, t - t_0) - \frac{q}{V}t_0$, where $v(x, t)$ is a solution of the problem

$$Lv(x) = -\frac{\partial v}{\partial t}, \quad x \in \Omega, \quad t > 0$$

$$\frac{\partial v}{\partial \vec{\nu}}|_{\Gamma_e} = 0,$$

$$v|_{\Gamma_w} = 0,$$

$$v(x, 0) = qu_1(x).$$

The diffusive capacity $J(u, t) = J(v, t)$. Function $v(x, t)$ is defined by

$$v(x, t) = \sum_{n=0}^{\infty} c_k \phi_k(x) e^{-\lambda_k t},$$

where $c_k = q \int_{\Omega} u_1(x) \phi_k dx$. Using integration by parts, we obtain

$$\int_{\Omega} Lu_1 \phi_k = \int_{\Omega} u_1 L \phi_k.$$

Hence,

$$\frac{1}{V} \int_{\Omega} \phi_k = \lambda_k \int_{\Omega} u_1 \phi_k.$$

Thus, for any $k = 1, 2, \dots$, $d_k c_k > 0$ and (5.34) implies that $J(u, t) \searrow J_{II}$. In other words, when the regime of production changes from pseudo-steady-state i. e. constant flow rate, to constant wellbore pressure the productivity index monotonically decreases to the boundary-dominated PI.

Example 2. For the purposes of analysis it is frequently assumed that at $t = 0$ the pressure in the reservoir is distributed uniformly, i. e., $u_0(x) = u_i$, where u_i is a positive constant. Then $c_k = u_i d_k$ and the productivity index is monotonically decreasing to the boundary-dominated PI.

Finally, consider an example of the initial pressure distribution yielding the productivity index which is less than the boundary dominated PI.

Example 3. Let $u_0(x) = 100\phi_0(x) - 3\phi_1(x)$. Then the diffusive capacity $J(u, t) < \lambda_0 V$.

An example of such initial distribution for an ideal cylindrical reservoir with vertical fully penetrated well is given in Fig.3, where the radial profile of $u_0(r)$ is given. The dimensionless radius of the reservoir is equal to $R_D = 1000$. Physically this example may be interpreted as follows: assume that the reservoir has been depleted by a set of wells. Suppose that the old wells are shut down and a new well is drilled and produced. Then the productivity index of the new well will monotonically increase to the boundary-dominated productivity index value.

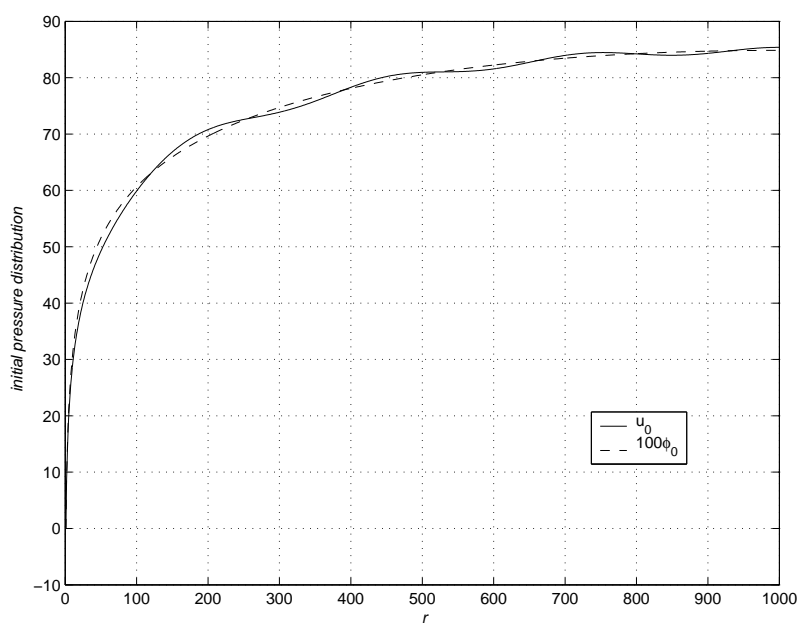


Fig. 3. Radial Profile of an Initial Distribution Yielding Small Diffusive Capacity.

CHAPTER VI

MODEL OF THE SKIN EFFECT

Stabilized production with constant rate is characterized by the pseudo-steady-state productivity index. When the well is damaged, the value of the productivity index is less than what is predicted by the model. As described in Literature Review, such effect is called thin-skin effect. In order to take into account the skin effect, the pseudo-steady-state productivity index is corrected according to the equation:

$$PI_{PSS,skin} = \frac{1}{\frac{1}{PI_{PSS}} + s}, \quad (6.1)$$

where s is the so-called *skin factor* or simply *skin*. As mentioned in Literature Review the skin effect can be modeled by a third type boundary condition specified on the well boundary [29], [16]. The well boundary condition in dimensionless form is then the following:

$$(p_D(r_D, t) - p_{Dw}(t))|_{r_D \rightarrow r_{Dw}} = sq_D. \quad (6.2)$$

Here, $p_D(r_D, t)$ is the pressure in the reservoir with a circular well of radius r_{Dw} , $p_{Dw}(t)$ is the flowing bottom hole pressure and q_D is the constant volumetric flow rate from the well. From here and below, we will omit the subscript “D”, although it is implied that all variables and functions are non-dimensionalized appropriately.

The skin factor concept was originally introduced to describe the behavior of damaged wells. Others have extended the idea to stimulated wells which have a higher productivity index than the pseudo-steady-state productivity index of an ideal well. In [19] it was shown that a negative skin s corresponds to a stimulated well.

All existing results on modeling the skin effect pertain to the constant rate production regime. In this section it will be shown that for the constant wellbore pressure production regime, the skin effect can be modeled by a third-type boundary condition

specified on the well boundary.

A. Diffusive Capacity for IBVP III in an Annulus

Let $u(r, t)$ be a solution of the problem

$$\frac{\partial}{\partial r} \left(r \frac{\partial u}{\partial r} \right) = \frac{\partial u}{\partial t}, \quad 1 < r < R_D, \quad , t > 0, \quad (6.3)$$

$$\frac{\partial u}{\partial r} \Big|_{r=R_D} = 0, \quad (6.4)$$

$$(u + \alpha \frac{\partial u}{\partial r}) \Big|_{r=1} = 0, \quad (6.5)$$

$$u(r, 0) = u_0(r). \quad (6.6)$$

Problem (6.3)-(6.6) models the axisymmetric flow of oil in an ideal isolated circular reservoir with a perfect circular well situated in the center. Here, $u(r, t)$ is the dimensionless pressure in the reservoir, the dimensionless formation permeability is 1 and the dimensionless outer radius is equal to R_D . The dimensionless wellbore radius is equal to 1. Constant wellbore pressure production is assumed. The thin skin zone adjacent to the well has a permeability below than that of the formation.

We will call a production regime for a well with a thin skin zone characterized by a constant productivity index a *generalized boundary-dominated state*. When $\alpha = 0$ (no damaged zone around the well), it is a boundary-dominated regime.

Along with problem (6.3)-(6.6), consider a related Sturm-Liouville problem:

$$\frac{\partial}{\partial r} \left(r \frac{\partial \phi_k^\alpha}{\partial r} \right) = -\lambda_k^\alpha \phi_k^\alpha, \quad 1 < r < R_D, \quad , t > 0, \quad (6.7)$$

$$\frac{\partial \phi_k^\alpha}{\partial r} \Big|_{r=R_D} = 0, \quad (6.8)$$

$$(\phi_k^\alpha + \alpha \frac{\partial \phi_k^\alpha}{\partial r}) \Big|_{r=1} = 0, \quad (6.9)$$

Let λ_0^α be the minimal nonnegative eigenvalue of the problem (6.7)-(6.9). If the

initial condition $u_0(r) = \phi_0^\alpha$ - corresponding to λ_0^α eigenfunction, then by propositions 3 and 4 of chapter Time Independent Diffusive Capacity, the generalized boundary-dominated productivity index is determined by $J_{III}(\alpha) = \lambda_0^\alpha V$ and $J_{III}(0) = J_{II}$.

In analogy to (6.1), we will defined the skin factor s by

$$s = s(\alpha) := \frac{1}{J_{III}(\alpha)} - \frac{1}{J_{II}} = \frac{1}{J_{III}(\alpha)} - \frac{1}{J_{III}(0)}, \quad (6.10)$$

Positive skin defined by (6.10) is an evidence of the damaged well. By analogy, the generalized boundary-dominated index of a stimulated well should be greater than the boundary-dominated index, yielding negative skin s .

When $\alpha < 0$, λ_0^α is the first positive eigenvalue. The eigenpair solves known equations involving Bessel functions of the first and the second kind [26]. Using known facts from the theory of Bessel functions, it is not hard to show the following.

Proposition 8. *As $\alpha \rightarrow \infty$, $\lambda_0^\alpha \rightarrow 0$. As $\alpha \rightarrow -\infty$, $\lambda_0^\alpha \rightarrow \lambda_0^{(N)}$ - where $\lambda_0^{(N)}$ is the minimal nontrivial eigenvalue of the following problem:*

$$\frac{\partial}{\partial r} \left(r \frac{\partial u}{\partial r} \right) = \frac{\partial u}{\partial t}, \quad 1 < r < R_D, \quad , t > 0, \quad (6.11)$$

$$\frac{\partial u}{\partial r} \Big|_{r=R_D} = 0, \quad (6.12)$$

$$\frac{\partial u}{\partial r} = 0, \quad (6.13)$$

$$u(r, 0) = u_0(r). \quad (6.14)$$

This implies, in particular, that $s(\alpha)$, defined by Eq.(6.10), is bounded from below, since $\lambda_0^{(N)}$ is bounded from above. The relation between s and α for $R_D = 1000$ and $R_D = 1000$ is shown in Figs. 4 and 5 for a range of values of α . The behavior of the constant diffusive capacity $J_{III}(\alpha)$ with respect to changes in α is demonstrated in Figs. 6 and 7. Figs. 4 and 5 illustrate that when $\alpha > 0$, skin $s = \alpha$, i.e., the

positive skin can be successfully modeled by the third type boundary condition, in perfect agreement with the constant rate case. In order to analyze the case of $\alpha < 0$, additional considerations are necessary.

Eigenfunctions ϕ_0^α corresponding to the minimal positive eigenvalue λ_0^α of the problem (6.7)-(6.9) for two sample positive and negative values of α are pictured in Figs. 8 and 9. As seen in Fig. 8, for negative α the corresponding eigenfunction ϕ_0^α changes sign on the interval $1 < r < R_D$. Recall that the initial condition of the problem (6.3)- (6.6) u_0 is equal to ϕ_0^α . Consequently, the sufficient condition for the generalized boundary-dominated state is such that the initial pressure distribution in the reservoir is not everywhere positive. Thus, a negative value of the skin factor s creates a physical contradiction, therefore problem (6.3)-(6.6) with $\alpha < 0$ can not serve as an appropriate model for a stimulated well.

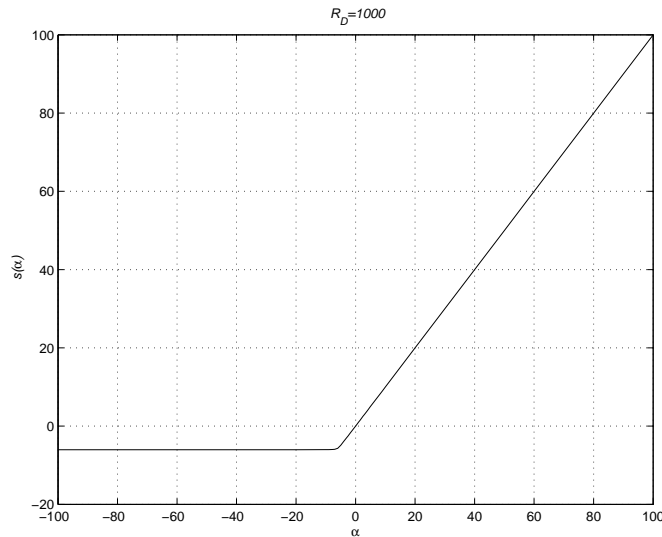


Fig. 4. Graph of $s(\alpha)$ for $R_D = 1000$.

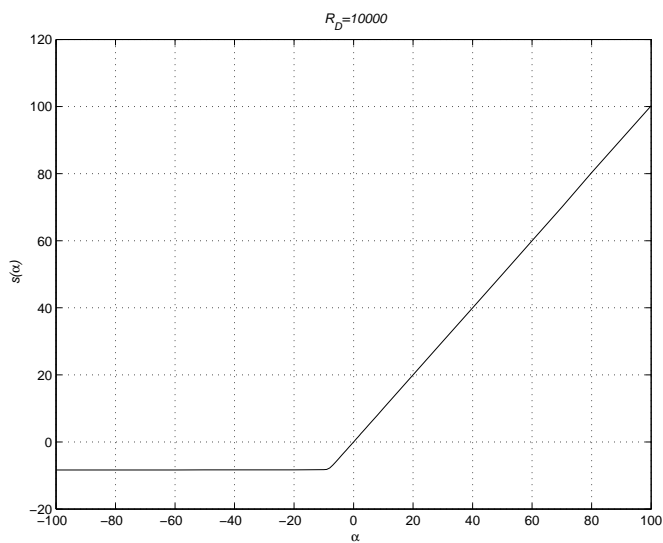


Fig. 5. Graph of $s(\alpha)$ for $R_D = 10000$.

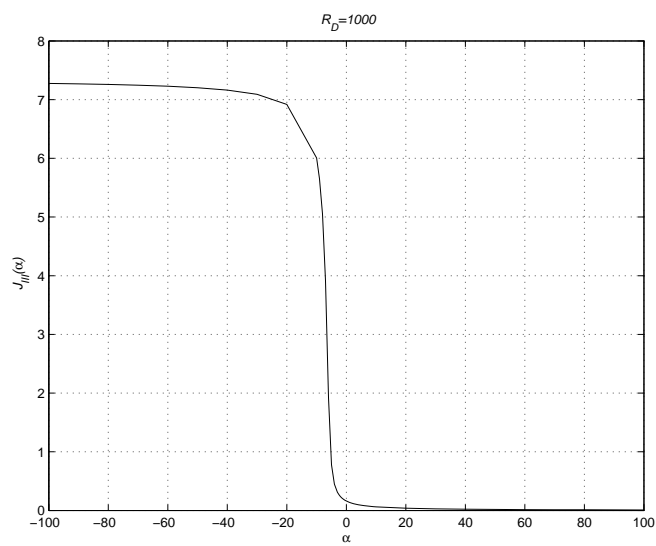


Fig. 6. Graph of $J_{III}(\alpha)$ for $R_D = 1000$.

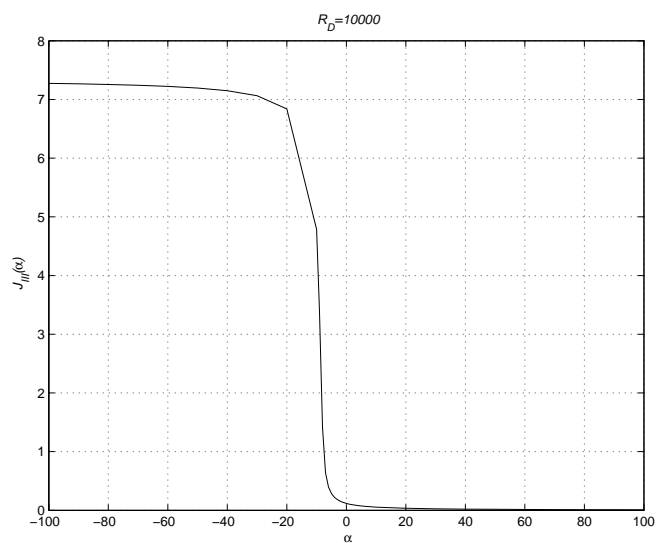


Fig. 7. Graph of $J_{III}(\alpha)$ for $R_D = 10000$.

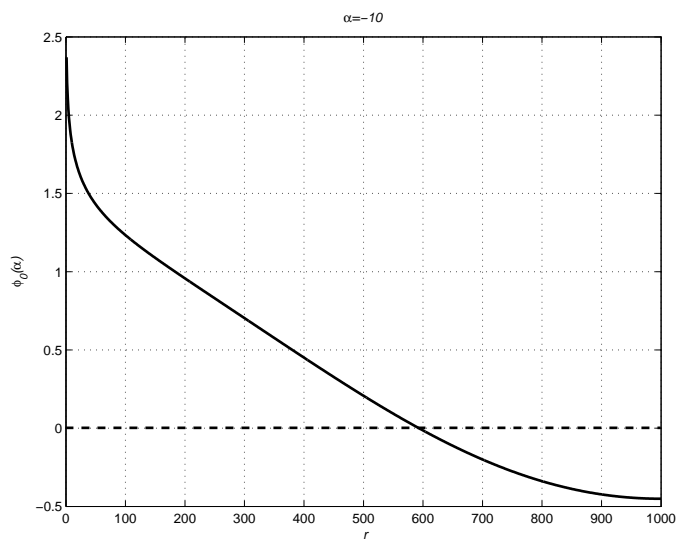


Fig. 8. Eigenfunction for Negative α . $R_D = 1000$.

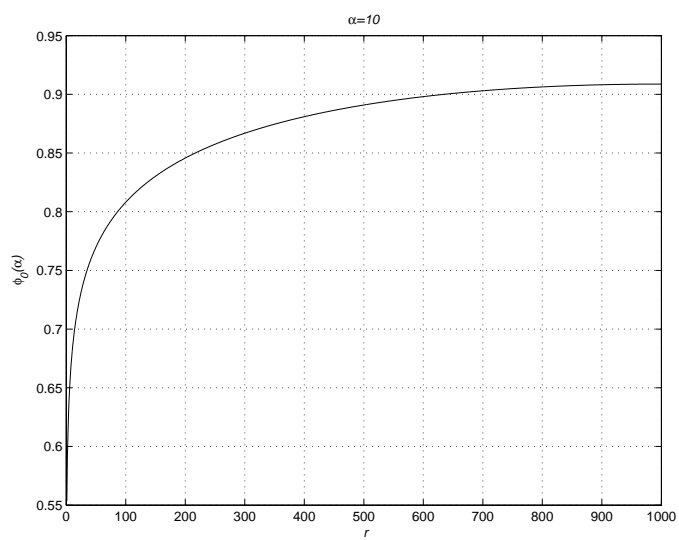


Fig. 9. Eigenfunction for Positive α . $R_D = 1000$.

CHAPTER VII

PRODUCTIVITY INDEX IN A TWO-DIMENSIONAL RESERVOIR

In this chapter we present a numerical investigation of the diffusive capacity/productivity index in two-dimensional domains. The formulas for pseudo-steady state and boundary dominated productivity indices derived in the chapter Time Independent Diffusive Capacity will be compared to the values obtained by Dietz' equation (3.12) for domains in which equation (3.12) can be applied. Then, using the new method we will evaluate the diffusive capacity in domains with more complex geometry, revealing some geometric characteristics of the domain that lead to the nonnegligible difference between J_I and J_{II} . The impact of anisotropy of the permeability will be analyzed too. We will restrict our attention to pseudo-steady-state and boundary-dominated productivity indices only, that is we will consider only initial boundary value problems I and II.

If the thickness of the reservoir is uniform, then for a fully penetrated vertical well the three-dimensional problem reduces to a two-dimensional one. Since the radius of wellbore is small compared to the dimensions of the reservoir, we can assume that the pressure is uniformly distributed on the wellbore. Therefore, for a two-dimensional problem, the pseudo-steady-state productivity index is equal to J_I given by equation (4.7).

Under the assumption that the reservoir is ideal and the well is perfectly circular, vertical and fully penetrated, the initial boundary value problems I and II can be formulated in terms of dimensionless variables as follows. Let $\Omega \in \mathbb{R}^2$ is the horizontal cross-section of such a reservoir. Let $\{r, \theta\}$ is a polar coordinate system specified on Ω along with the cartesian coordinate system $\{x, y\}$. The origins of both coordinate systems are located at the center of the well, which is represented by a circle with

equation $r = 1$. Let R_D be the radius of the circle of the same area as Ω . Then the dimensionless area V of Ω is equal to $(R_D^2 - 1)/2$. As before, let Γ_e denote the exterior boundary of Ω . The auxiliary steady-state problem (4.3)-(4.5) and the Sturm-Liouville problem (4.24)-(4.26) can be written as:

$$\frac{\partial^2 u_1}{\partial x^2} + \frac{\partial^2 u_1}{\partial y^2} = -\frac{1}{V} \quad (7.1)$$

$$u_1|_{r=1} = 0 \quad (7.2)$$

$$\frac{\partial u_1}{\partial \vec{n}}|_{\Gamma_e} = 0. \quad (7.3)$$

and

$$\frac{\partial^2 \phi_0}{\partial x^2} + \frac{\partial^2 \phi_0}{\partial y^2} = -\lambda_0 \phi_0, \quad (7.4)$$

$$\phi_0|_{r=1} = 0 \quad (7.5)$$

$$\frac{\partial \phi_0}{\partial \vec{n}}|_{\Gamma_e} = 0, \quad (7.6)$$

respectively. By propositions 1 and 2, the values of the pseudo-steady state and boundary dominated productivity indices are given by the following equations, respectively:

$$J_I = \frac{V}{\int_{\Omega} u_1 dx} \quad (7.7)$$

and

$$J_{II} = \lambda_0 V. \quad (7.8)$$

For all two-dimensional domains considered in this section, problems (7.1)-(7.3) and (7.4)-(7.6) were solved in PDE toolbox of MATLAB software package. The chapter Remarks on Numerical Calculations provides a sample code and some considerations on the precision of algorithms related to the finite element approximation used in this software.

A. Comparison to Existing Results

Tables 1 and 2 provide the numerical results for a variety of the two dimensional drainage area shapes. The notations used in the table are the following: J_I is the constant diffusive capacity of the initial boundary value problem I (pseudo-steady-state productivity index) computed by Eq. (7.7). Value J_I is compared to the value of the pseudo-steady-state productivity index J_{PSS} computed by Eq.(3.12) with the shape factors C_A taken from [7] for every considered shape. The constant diffusive capacity J_{II} , given by Eq.(7.8), is compared to the productivity index J_{BD} computed by Eq. (3.12) with the boundary-dominated shape factors C_A provided in [17]. Note that shape factors for some of the drainage area shapes considered in [7] are not provided in [17]. The results are presented for two values of the dimensionless radius R_D of the drainage area, $R_D = 1000$ and $R_D = 10000$, since it is conventionally considered that for a single vertical well, the drainage area that it can deplete is most likely to fall within the range specified by these values of the dimensionless radius.

As illustrated by the tables, Eqs.(7.7) and (7.8) closely agree to the corresponding existing formulas. The largest difference between the corresponding values is the one between J_I and J_{II} in the drainage areas where the well is located far from the center of symmetry of the domain.

As noted before, one of the disadvantages of Eq.(3.12) is that it cannot be applied to the drainage area shapes that do not satisfy the requirements of the method of images. On the other hand, the method of deriving Eq.3.12 allowed the authors to compute the time of the onset of the pseudo-steady-state [24]. In the derivation of Eqs. (7.7) and (7.8), it is assumed that the productivity index is constant starting from $t = 0$, thus excluding the possibility to estimate the time required for stabilization of the productivity index. However, Eq.(7.7) and (7.8) are valid for all drainage area

shapes and can be applied to a general reservoir without the usual assumptions of the homogeneity and isotropy of the media. In the next sections we exploit these useful features of the new formulas for productivity index to analyze its behavior in more complex geometries and for anisotropic media.

Table 1.: Productivity Indices for Typical Drainage Area Shapes. Part 1.

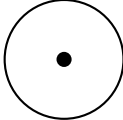
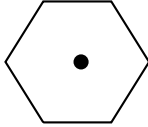
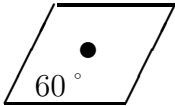
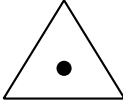
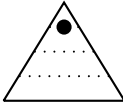
Shape	$R_D = 1000$				
	J_I	J_{II}	$ \frac{J_I - J_{II}}{J_{II}} $, percent	$ \frac{J_I - J_{PSS}}{J_I} $, percent	$ \frac{J_{II} - J_{BD}}{J_{II}} $, percent
	0.1620	0.1626	0.38	n/a	0.03
	0.1619	0.1625	0.41	n/a	0.09
	0.1593	0.1606	0.58	n/a	0.26
	0.1598	0.1609	0.50	n/a	0.15
	0.1566	0.1578	0.76	n/a	0.07

Table 1.: (continued)

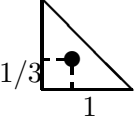
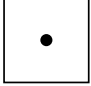
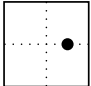
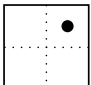
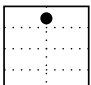
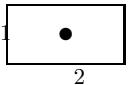
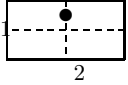
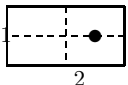
Shape	$R_D = 1000$				
	J_I	J_{II}	$ \frac{J_I - J_{II}}{J_{II}} $, percent	$ \frac{J_I - J_{PSS}}{J_I} $, percent	$ \frac{J_{II} - J_{BD}}{J_{II}} $, percent
	0.1069	0.1107	3.51	n/a	0.08
	0.1615	0.1622	0.41	0.08	0.08
	0.1496	0.1516	1.27	0.09	0.02
	0.1376	0.1403	1.97	0.09	0.14
	0.1351	0.1374	1.69	0.08	0.18
	0.1567	0.1578	0.68	0.12	0.08
	0.1482	0.1495	0.91	0.14	0.06
	0.1351	0.1403	3.73	0.34	0.04

Table 1.: (continued)

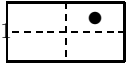
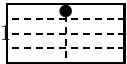
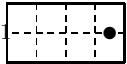
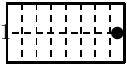

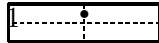
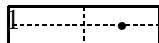
Shape	$R_D = 1000$				
	J_I	J_{II}	$ \frac{J_I - J_{II}}{J_{II}} $, percent	$ \frac{J_I - J_{PSS}}{J_I} $, percent	$ \frac{J_{II} - J_{BD}}{J_{II}} $, percent
 2	0.1283	0.1331	3.59	0.32	0.06
 2	0.1355	0.1369	1.00	0.13	0.06
 2	0.1065	0.1227	13.22	8.64	0.03
 2	0.0990	0.1114	11.16	6.84	0.02
 4	0.1394	0.1421	1.90	0.31	0.07
 4	0.1329	0.1354	1.84	0.29	0.06
 4	0.1047	0.1161	9.88	1.06	0.04

Table 1.: (continued)

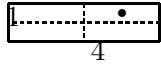
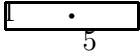
Shape	$R_D = 1000$				
	J_I	J_{II}	$ \frac{J_I - J_{II}}{J_{II}} $, percent	$ \frac{J_I - J_{PSS}}{J_I} $, percent	$ \frac{J_{II} - J_{BD}}{J_{II}} $, percent
	0.1013	0.1116	9.22	0.85	0.06
	0.1307	0.1342	2.63	0.44	0.06

Table 2.: Productivity Indices for Typical Drainage Area Shapes. Part 2.

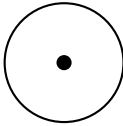
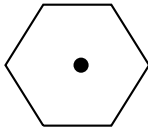
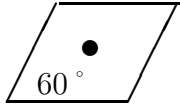
Shape	$R_D = 10000$				
	J_I	J_{II}	$ \frac{J_I - J_{II}}{J_{II}} $, percent	$ \frac{J_I - J_{PSS}}{J_I} $, percent	$ \frac{J_{II} - J_{BD}}{J_{II}} $, percent
	0.1180	0.1183	0.20	n/a	0.05
	0.1180	0.1183	0.20	n/a	0.05
	0.1167	0.1173	0.31	n/a	0.17

Table 2.: (continued)

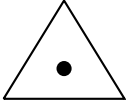
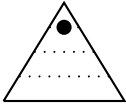
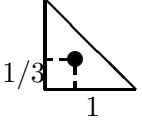
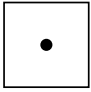
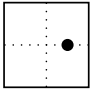
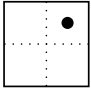
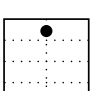
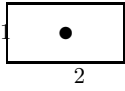
Shape	$R_D = 10000$				
	J_I	J_{II}	$ \frac{J_I - J_{II}}{J_{II}} $, percent	$ \frac{J_I - J_{PSS}}{J_I} $, percent	$ \frac{J_{II} - J_{BD}}{J_{II}} $, percent
	0.1170	0.1173	0.27	n/a	0.10
	0.1153	0.1158	0.40	n/a	0.03
	0.0863	0.0883	2.25	n/a	0.07
	0.1179	0.1181	0.21	0.16	0.04
	0.1116	0.1124	0.69	0.34	0.00
	0.1049	0.1061	1.12	0.47	0.09
	0.1034	0.1044	0.96	0.40	0.12
	0.1153	0.1157	0.37	0.30	0.04

Table 2.: (continued)

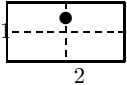
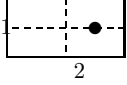
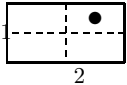
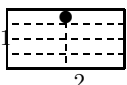
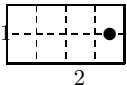
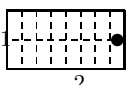

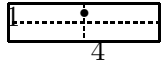
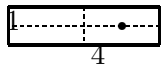
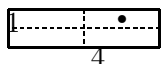
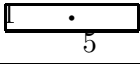
Shape	$R_D = 10000$				
	J_I	J_{II}	$ \frac{J_I - J_{II}}{J_{II}} $, percent	$ \frac{J_I - J_{PSS}}{J_I} $, percent	$ \frac{J_{II} - J_{BD}}{J_{II}} $, percent
 2	0.1107	0.1112	0.50	0.43	0.03
 2	0.1038	0.1061	2.11	2.03	0.02
 2	0.0998	0.1019	2.09	2.03	0.03
 2	0.1040	0.1041	0.58	0.52	0.03
 2	0.0862	0.0957	9.94	9.87	0.01
 2	0.0811	0.0887	8.51	8.44	0.00
 4	0.1059	0.1071	1.08	1.01	0.03

Table 2.: (continued)

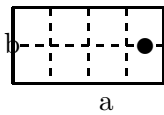
Shape	$R_D = 10000$				
	J_I	J_{II}	$ \frac{J_I - J_{II}}{J_{II}} $, percent	$ \frac{J_I - J_{PSS}}{J_I} $, percent	$ \frac{J_{II} - J_{BD}}{J_{II}} $, percent
	0.1021	0.1032	1.07	1.00	0.03
	0.0859	0.0917	6.26	6.19	0.02
	0.0836	0.0888	5.92	5.87	0.03
	0.1010	0.1025	1.53	1.47	0.03

B. Productivity Index in Non-symmetric Domains

It is a belief in the reservoir engineering community that the two characteristics of a well capacity cannot differ significantly. Tables 1 and 2 confirm that in simple polygonal domains with the well located in the center of symmetry, J_I and J_{II} don't differ from each other by more than 10%. However, upon inspection of Tables 1 and 2 we can identify certain geometrical characteristics of the drainage area that can have an effect on the difference between J_I and J_{II} (pseudo-steady-state and boundary-dominated productivity indices). Two such geometrical characteristics are the symmetry of the domain about the well and the shape of the exterior boundary.

We consider a rectangular drainage area corresponding to $R_D = 1000$ with aspect ratio of sides a/b . The well is located at $(\frac{7}{8}a, \frac{1}{2}b)$ inside the rectangle. Table 3 illustrates that the difference between J_I and J_{II} becomes significantly large for $k \geq 10$.

Table 3.: The Effect of the Location of the Well Relative to the Center of Gravity on the Difference Between BD and PSS PI's.

	a/b	J_I	J_{II}	$ \frac{J_I - J_{II}}{J_{II}} $, percent
	2	0.1227	0.1065	4.69
	10	0.0539	0.4370	23.34
	50	0.0137	0.0100	37.00
	100	0.0071	0.0050	39.22
	500	0.0014	0.0010	40.58
	1000	0.0007	0.0005	41.02

C. Productivity Index in Domains Violating Isoperimetric Inequality

Theorem 1 of chapter Time Independent Diffusive Capacity gives the means to investigate deeper the effects on the difference between J_I and J_{II} of the shape of the exterior boundary of the domain. The difference between J_I and J_{II} is expected to be greater when the constant C_Ω on the right hand side of the inequality (4.39) is much greater than 1. The constant C_Ω is, in its turn, determined by the minimal

eigenvalue λ_0 and the behavior of the corresponding eigenfunction ϕ_0 of the elliptic problem (7.4)- (7.6).

The first eigenpair of the problem is directly related to the geometry of the domain, namely, to the symmetry and curvature of the exterior boundary and the shape of the well boundary. To illustrate the effect of the curvature and the symmetry of the exterior boundary, consider domains which violate the isoperimetric inequality.

Let Ω be a domain in an n -dimensional space, Σ an $(n-1)$ - dimensional hypersurface, dividing Ω into the two parts A and $\Omega \setminus A$. Ω is said to satisfy the isoperimetric inequality, if there exists constant α_p such that for any hypersurface Σ the following holds:

$$mes_{n-1}(\Sigma) \geq \alpha_p \min\{mes_n(A), mes_n(\Omega \setminus A)\}^{\frac{n-1}{n}}. \quad (7.9)$$

If the domain does not satisfy the isoperimetric inequality (7.9), then the Friedrich's inequality does not hold on the domain [25]. Therefore, the first eigenvalue of the problem (7.4)-(7.6) can be negligibly small, making the difference between J_I and J_{II} significant.

It is not hard to show that for $0 < \epsilon < 1$, both domains pictured in Figs. 10 and 11 violate the isoperimetric inequality. For either shape, the domain parameters b and ϵ change so that the ratio of the area of the domain to the radius of the well is held constant and corresponds to $R = 1000$. The circular well is located in the center of gravity. The results of the numerical investigation for domains violating the isoperimetric inequality (7.9) are collected in Table 4. The symmetrical domain is presented in order to illustrate the importance of symmetry: the difference between J_I and J_{II} for a symmetrical domain is significantly less than for a nonsymmetrical domain with the same curvature of the exterior boundary.

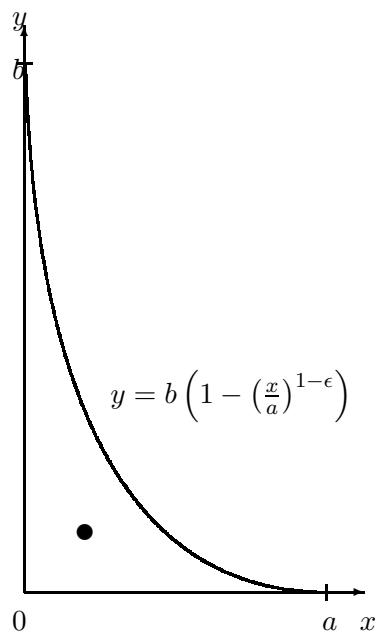


Fig. 10. Domain with a Violated Isoperimetric Inequality.

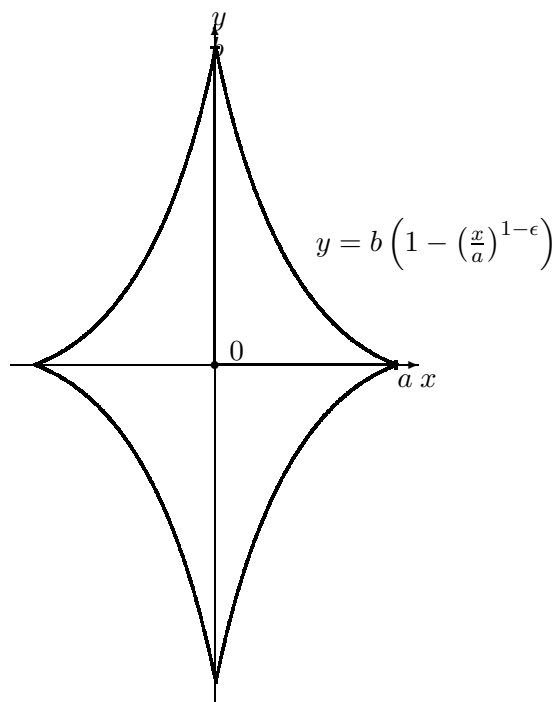


Fig. 11. Symmetrical Domain with a Violated Isoperimetric Inequality.

Table 4.: The Effect of Isoperimetric Inequality and Symmetry of the Domain on the Difference Between J_I and J_{II} .

Shape	ϵ	J_I	J_{II}	$ \frac{J_I - J_{II}}{J_{II}} $, percent
see Fig.10	0.0	0.1227	0.1065	4.69
	0.4	0.0539	0.4370	23.34
	0.6	0.0137	0.0100	37.00
	0.8	0.0071	0.005	39.22
see Fig.11	0.8	0.0990	0.1222	19.00
	0.95	0.0056	0.0311	82.00

D. Orthotropic Media

It is generally agreed that porous media exhibits directinal properties. In such material, if the tensor of permeability is self-conjugate, then the directions of the maximum permeability and minimal permeability are perpendicular to each other [29]. Such material is called *orthotropic* [29]. Assume that the porous media is homogeneous and orthotropic. If x - and y -axes are collinear with the directions of the maximal and minimal (or vice versa) permeabilities, then the coefficient matrix A in (4.24)-(4.26) is diagonal. Let $k = k_y/k_x$, where k_x and k_y are the components of A corresponding to x and y directions respectively. Then the boundary value problem (7.1)- (7.3) and the Sturm-Liouville problem (7.4)-(7.6) must be rewritten accordingly:

$$\frac{\partial^2 u_1}{\partial x^2} + k \frac{\partial^2 u_1}{\partial y^2} = -\frac{1}{V} \quad (7.10)$$

$$u_1|_{r=1} = 0 \quad (7.11)$$

$$\frac{\partial u_1}{\partial \vec{\nu}}|_{\Gamma_e} = 0. \quad (7.12)$$

and

$$\frac{\partial^2 \phi_0}{\partial x^2} + k \frac{\partial^2 \phi_0}{\partial y^2} = -\lambda_0 \phi_0, \quad (7.13)$$

$$\phi_0|_{r=1} = 0 \quad (7.14)$$

$$\frac{\partial \phi_0}{\partial \vec{\nu}}|_{\Gamma_e} = 0. \quad (7.15)$$

The profound effect of anisotropy of the medium on the difference between J_I and J_{II} is illustrated in Table 5. For regular drainage shapes, the effect of the anisotropy becomes evident for $k_y/k_x = 50$. The domains violating the isoperimetric inequality are included to illustrate an interesting interplay between the two effects, one - caused by the anisotropy of medium and another one - caused by the shape of the exterior boundary.

Table 5.: The Effect of Anisotropy on the Difference
Between J_I and J_{II} .


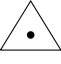
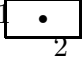
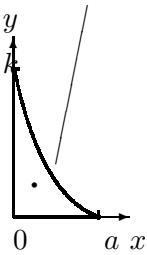
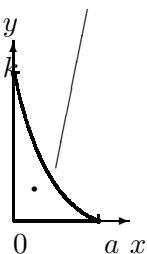
Shape	k	$R_D = 10000$					
		J_{II}	J_I	$ \frac{J_I - J_{II}}{J_{II}} $, percent	$\max_{\Omega} \phi_0$	$\bar{\phi}_0$	C_{DC}
	1	0.1620	0.1626	0.39	0.0117	0.0114	1.0301
	10	0.4870	0.4934	1.29	0.0129	0.0116	1.1137
	20	0.6532	0.6683	2.26	0.0138	0.0119	1.1581
	50	0.9210	0.9650	4.56	0.0156	0.0125	1.2427
	100	1.1531	1.2441	7.32	0.0178	0.0133	1.3343
	1	0.1170	0.1173	0.27	0.0119	0.0127	1.0671
	10	0.3527	0.3564	1.05	0.0123	0.0147	1.1921
	20	0.4782	0.4873	1.88	0.0127	0.0160	1.2665
	50	0.6947	0.7234	3.98	0.0135	0.0191	1.4145
	100	0.9019	0.9680	6.83	0.0145	0.0230	1.5844
	1/10	0.0350	0.0354	1.13	0.0124	0.0159	1.2849
	1/20	0.0235	0.0240	2.10	0.0128	0.0182	1.4232
	1/50	0.0134	0.0140	4.66	0.0138	0.0238	1.7252
	1/100	0.0084	0.0092	8.38	0.0148	0.0316	2.1340
	1	0.1153	0.1158	0.37	0.0122	0.0130	1.0636
	10	0.3049	0.3119	2.25	0.0137	0.0161	1.1799
	20	0.3854	0.4000	3.67	0.0146	0.0180	1.2352
	50	0.4986	0.5324	6.34	0.0161	0.0212	1.3198
	100	0.5848	0.6420	8.91	0.0174	0.0242	1.3905

Table 5.: (continued)

Shape	k	$R_D = 10000$					
		J_{II}	J_I	$ \frac{J_I - J_{II}}{J_{II}} $, percent	$\max_{\Omega} \phi_0$	$\bar{\phi}_0$	C_{DC}
$y = k \left(1 - \left(\frac{x}{a}\right)^{0.8}\right)$ 	1	0.0971	0.0999	2.81	0.0100	0.0157	1.5707
	10	0.3680	0.3701	0.56	0.0096	0.0113	1.1773
	20	0.5327	0.5354	0.50	0.0095	0.0107	1.1302
	50	0.8653	0.8717	0.73	0.0094	0.0114	1.2109
	100	1.2604	1.2771	1.31	0.0094	0.0125	1.3267
	1/10	0.0178	0.0206	13.75	0.0100	0.0286	2.8675
	1/20	0.0097	0.0120	18.96	0.0094	0.0329	3.4851
	1/50	0.0041	0.0056	25.58	0.0085	0.0364	4.2922
	1/100	0.0021	0.0030	29.85	0.0078	0.0377	4.8229
$y = k \left(1 - \left(\frac{x}{a}\right)^{0.8}\right)$ 	1	0.0918	0.0958	4.23	0.0100	0.0189	1.9016
	10	0.3624	0.3651	0.75	0.0096	0.0121	1.2607
	20	0.5270	0.5302	0.61	0.0095	0.0112	1.1864
	50	0.8584	0.8652	0.78	0.0094	0.0115	1.2175
	100	1.2508	1.2677	1.33	0.0094	0.0126	1.3393
	1/10	0.0152	0.0189	19.26	0.0089	0.0351	3.9515
	1/20	0.0081	0.0108	25.07	0.0081	0.0382	4.7386
	1/50	0.0034	0.0049	31.55	0.0071	0.0402	5.6254
	1/100	0.0017	0.0027	35.39	0.0066	0.0408	6.1571

CHAPTER VIII

PRODUCTIVITY INDEX IN A THREE-DIMENSIONAL RESERVOIR

As described in Literature Review, the existing methods of evaluating the productivity index, have two major drawbacks. First, the evaluation of a productivity index requires solving a transient problem in a period of time long enough for the pressure to reach a pseudo-steady-state. When the well is not fully penetrated or directionally drilled (deviated or horizontal), the time period necessary for the pressure to stabilize may become excessively long, creating difficulties for computational procedures. Since the essence of reservoir engineering is the ability to adjust the parameters of the reservoir/well model in real time, it is a serious obstacle. To address the problem of the excessively long computations, some simplifying assumptions are made. Most of the methods are based on the assumption that the thickness of the reservoir is small enough to make the flow in the vertical direction negligible or so insignificant that its impact on the distribution of pressure can be included in a skin factor[22, 15]. Note that the skin factor in this setting is different from the thin skin factor described in the section Model of the Skin Effect.

With the restriction on the reservoir thickness, the problem reduces to a two-dimensional one. Then the techniques for two-dimensional reservoirs can be applied. The majority of such techniques utilizes the method of images, creating the second drawback - restrictions on the geometry of the domain.

With this in mind, a number of numerical experiments were conducted for various well configurations in three dimensional domains. The purpose of this part of the dissertation is to illustrate the behavior of the productivity indices in a general homogeneous three dimensional reservoir/well system. Eqs. (4.7) and (4.27) are convenient to use in such settings, since they only require solution of steady-state three

dimensional problems. Note that the use of Eq. (4.7) implies that we assume that in constant rate of production regime the pressure is uniformly distributed on the wellbore at each $t > 0$. One can argue that this assumption is physically realistic for horizontal wells of any length, if we assume that the wellbore has infinite conductivity so that the pressure of the fluid entering the wellbore instantly equalizes at every point of the wellbore. For vertical or slanted wells, the assumption of uniform pressure distribution on the wellbore at each $t > 0$ implies that we neglect the gravity effects. Certainly, for long vertical or slanted wells, such assumption is not physically realistic.

All the computations described in this section have been implemented in the software package FEMLAB. The section Remarks on Numerical Calculations provides some information and concerns related to the use of the software.

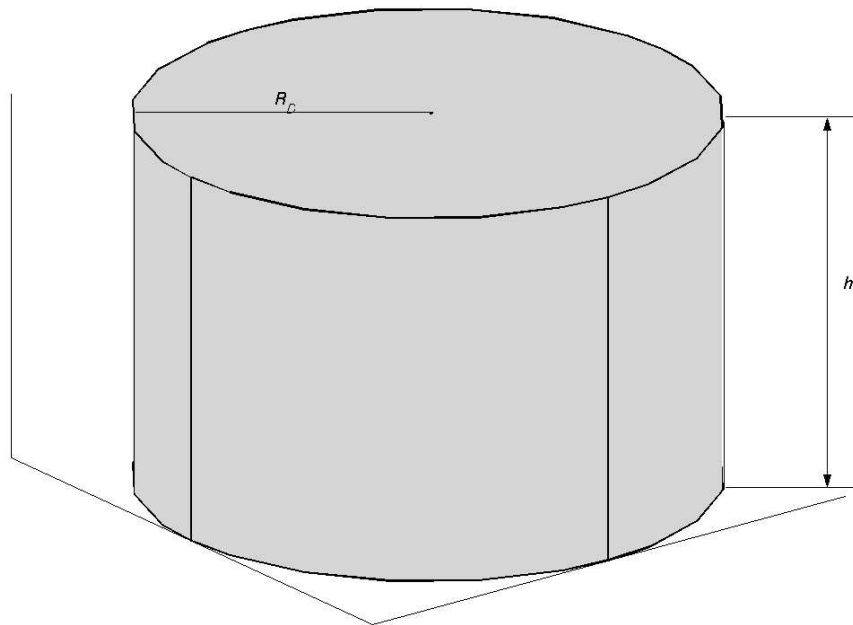


Fig. 12. Schematic Representation of Domain D_1 .

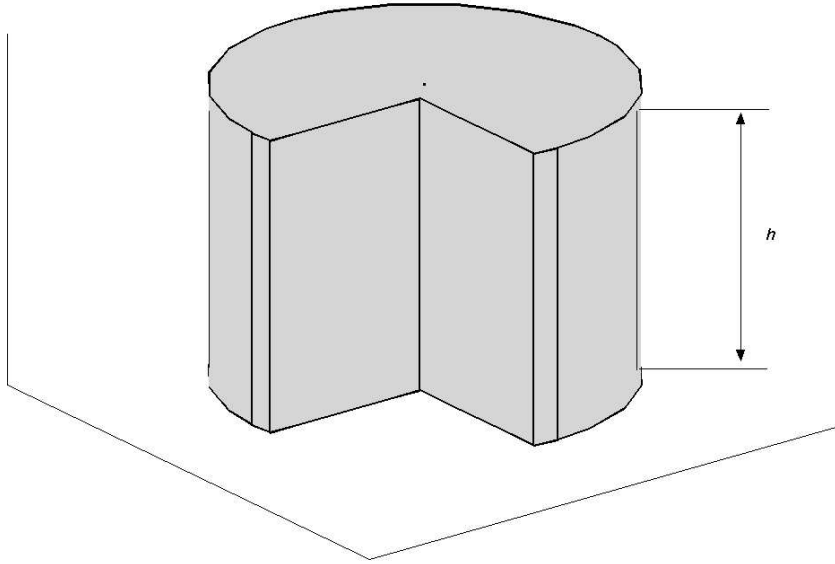


Fig. 13. Schematic Representation of Domain D_2 .

Two domains modeling three dimensional reservoirs that were considered for the numerical study are depicted in Figs.12, 13 and 14. Domain D_1 is a cylindrical reservoir of uniform thickness h and the dimensionless radius R_D . Analogously to the two-dimensional definition, R_D is defined as the ratio of the radius of the horizontal cross-section (in this case, circle) to the well radius. The value of R_D is set to 1000 for all settings.

Domain D_2 was chosen for illustration as a geometrical shape that is not appropriate for the method of images. Similarly to D_1 , domain D_2 is of uniform thickness h . Fig. 14 shows the horizontal cross-section of domain D_2 . The length of side c of the straight angle part extracted from the circle is chosen so that the area of the extraction constitutes $1/5$ of the area of the circle. For consistency of comparisons made below, the radius of the circle of the cross-section is chosen so that the remaining area is equal to the area of the cross-section of domain D_1 , i. e. the dimensional

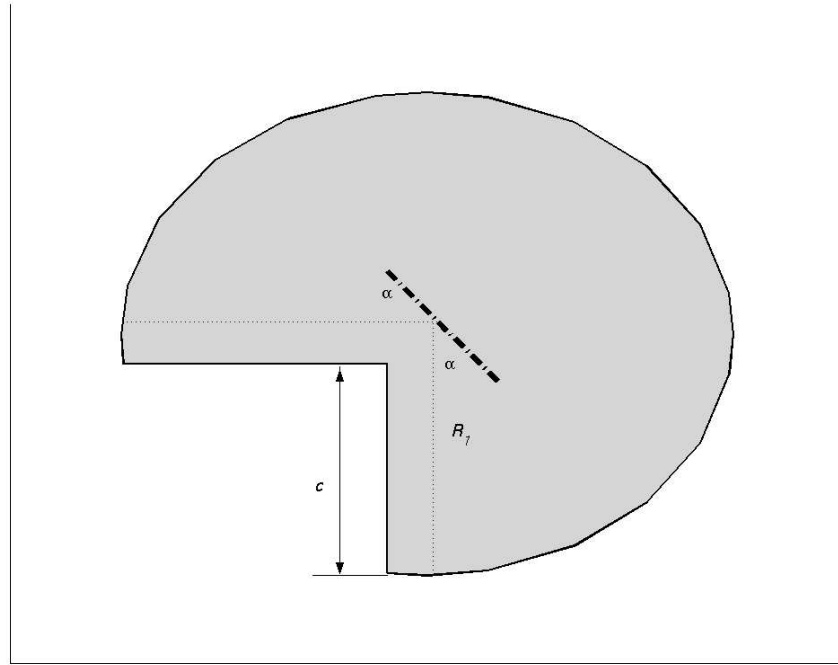


Fig. 14. Schematic Representation of Horizontal Projection of Domain D_2 .

radius associated with the horizontal cross-section of D_2 is $R_D = 1000$.

Several well configurations were considered for both reservoir models. For domain D_2 , the direction of any considered well was such that its projection on the top of the reservoir corresponded to the schematic configuration shown in Fig.14. A well is modeled by a circular cylinder with the dimensionless radius $r_w = 1$. Then for both domains D_1 and D_2 , the cross-section by the plane containing the well is a rectangle. Figs. 15, 16, 17, 18 and 19 show such cross-sections for every well configuration, considered in computational experiments. In configurations (A), (B), (D) and (E), the center of symmetry of the well coincides with the center of symmetry of the cross-section. In configuration (C), the well is drilled from the middle of the top side of the reservoir cross-section.

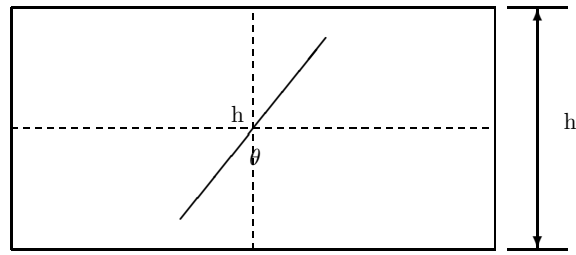


Fig. 15. Schematic Representation of the Vertical Cross-section for Well Configuration (A). See p. 66

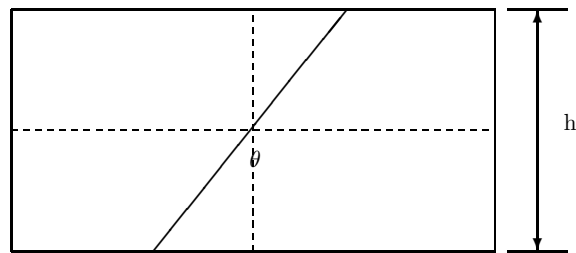


Fig. 16. Schematic Representation of the Vertical Cross-section for Well Configuration (B). See p. 66

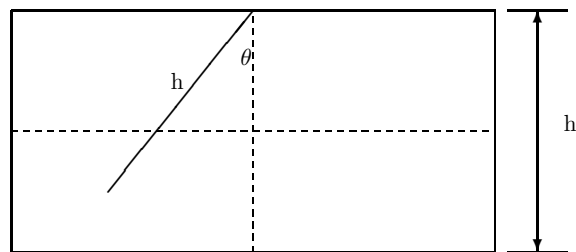


Fig. 17. Schematic Representation of the Vertical Cross-section for Well Configuration (C). See p. 66

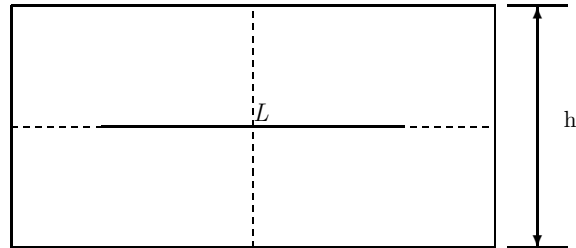


Fig. 18. Schematic Representation of the Vertical Cross-section for Well Configuration (D). See p. 66

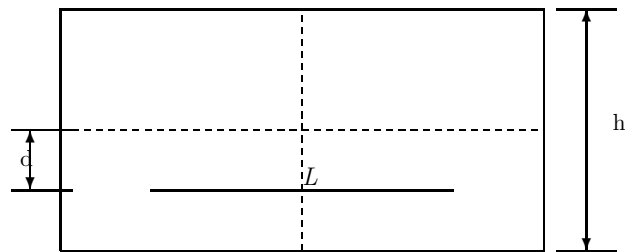


Fig. 19. Schematic Representation of the Vertical Cross-section for Well Configuration (E). See p. 66

A. Directionally Drilled Wells. Effect of Vertical Flow.

Tables 6 and 7 as well as Fig.20 illustrate the behavior of the pseudo steady state and boundary dominated indices for a directionally drilled fully penetrated well. The well passes through the center of symmetry of the reservoir cross-section for both domains. As expected, both J_I (pseudo-steady-state) and J_{II} (boundary-dominated) productivity indices increase with the length of penetration.

Table 8 and Fig.21 show how J_I and J_{II} change with direction of the well of the fixed length passing through the center of symmetry of the domain. Productivity indices for well configuration (C) for domains D_2 and D_1 are given in Tables 9 and 10, respectively. In all cases, the penetration length of the well is equal to h so that for $\theta = 0$, the vertical well fully penetrates the reservoir. The graphs of J_I and J_{II} as functions of the angle θ of the well direction, shown in Figs.22 and 23, reveal that the optimal direction of a well of the fixed penetration length is not the vertical one. It is a clear indication of the effect of the vertical flow of fluid from the bottom of the reservoir toward the slanted well. Clearly, this effect is impossible to quantify by a reduced two dimensional problem for a fully penetrated vertical well.

Table 6.: Productivity Indices for Domain D_1 , Well Configuration (B).

θ	0	15	30	45	60	75
J_I	0.1629	0.1662	0.1785	0.2019	0.2578	0.4015
J_{II}	0.1624	0.1656	0.1775	0.2006	0.2555	0.3930
$\frac{J_I - J_{II}}{J_{II}}$, percent	0.37	0.15	0.24	0.33	0.6	2.2

Table 7.: Productivity Indices for Domain D_2 , Well Configuration (B).

θ	0	15	30	45	60	75
J_I	0.1597	0.1603	0.1720	0.1947	0.2414	0.3650
J_{II}	0.1587	0.1596	0.1710	0.1931	0.2384	0.3556
$\frac{J_I - J_{II}}{J_{II}}$, percent	0.60	0.49	0.60	0.84	1.26	2.65

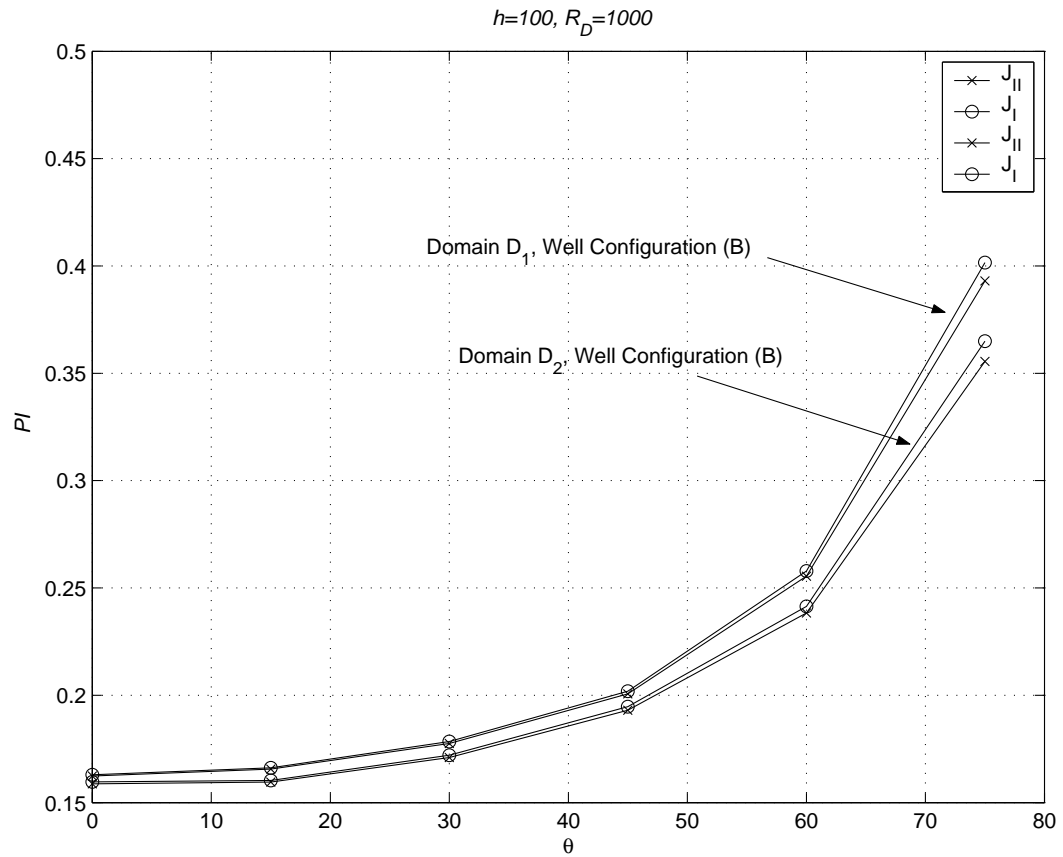


Fig. 20. Productivity Indices for Domains D_1 and D_2 for Well Configuration (B).

Table 8.: Productivity Indices for Domain D_1 , Well Configuration (A).

θ	0	15	30	45	60	75
J_I	0.1629	0.1841	0.1875	0.1800	0.1784	0.1780
J_{II}	0.1624	0.1831	0.1866	0.1796	0.1781	0.1772
$\frac{J_I - J_{II}}{J_{II}}$, percent	0.37	0.55	0.52	0.22	0.17	0.46

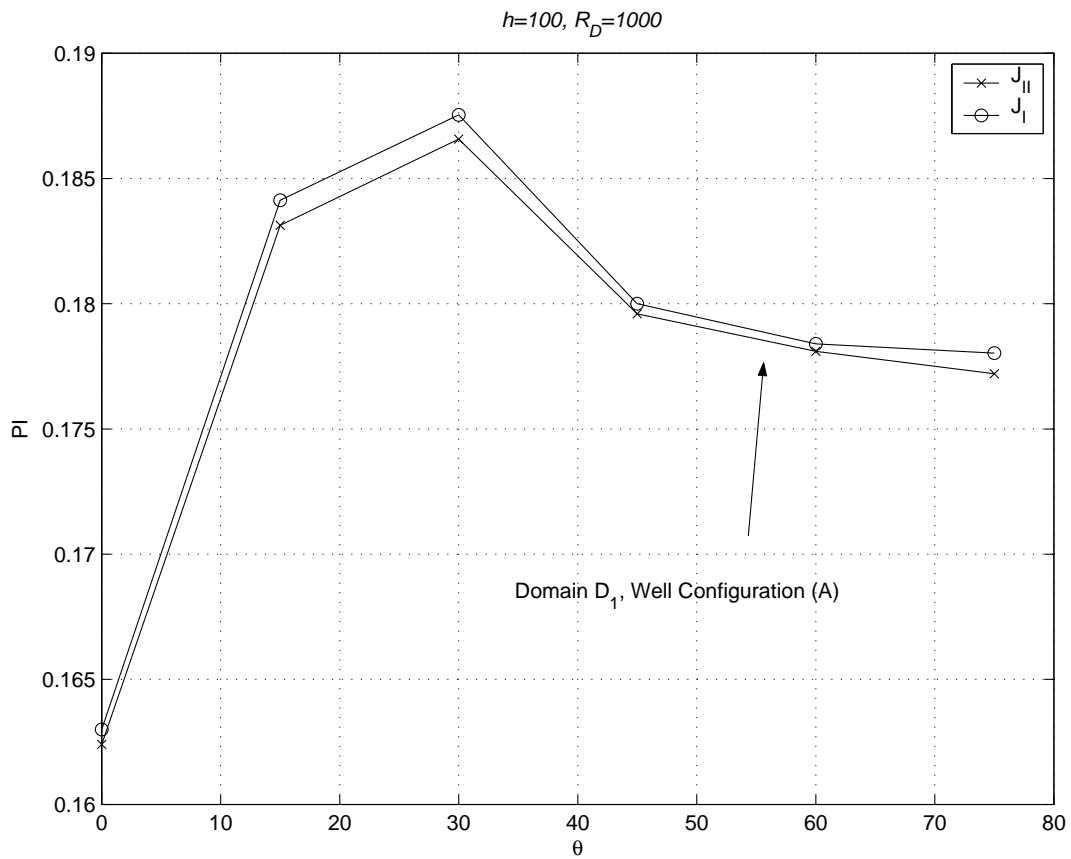


Fig. 21. Productivity Indices for Domain D_1 , Well Configuration (A).

Table 9.: Productivity Indices for Domains D_2 , Well Configuration (C).

θ	0	15	30	45	60	75
J_I	0.1597	0.1714	0.1673	0.1634	0.1586	0.1529
J_{II}	0.1587	0.1704	0.1662	0.1623	0.1576	0.1520
$\frac{J_I - J_{II}}{J_{II}}$, percent	0.60	0.64	0.64	0.67	0.61	0.59

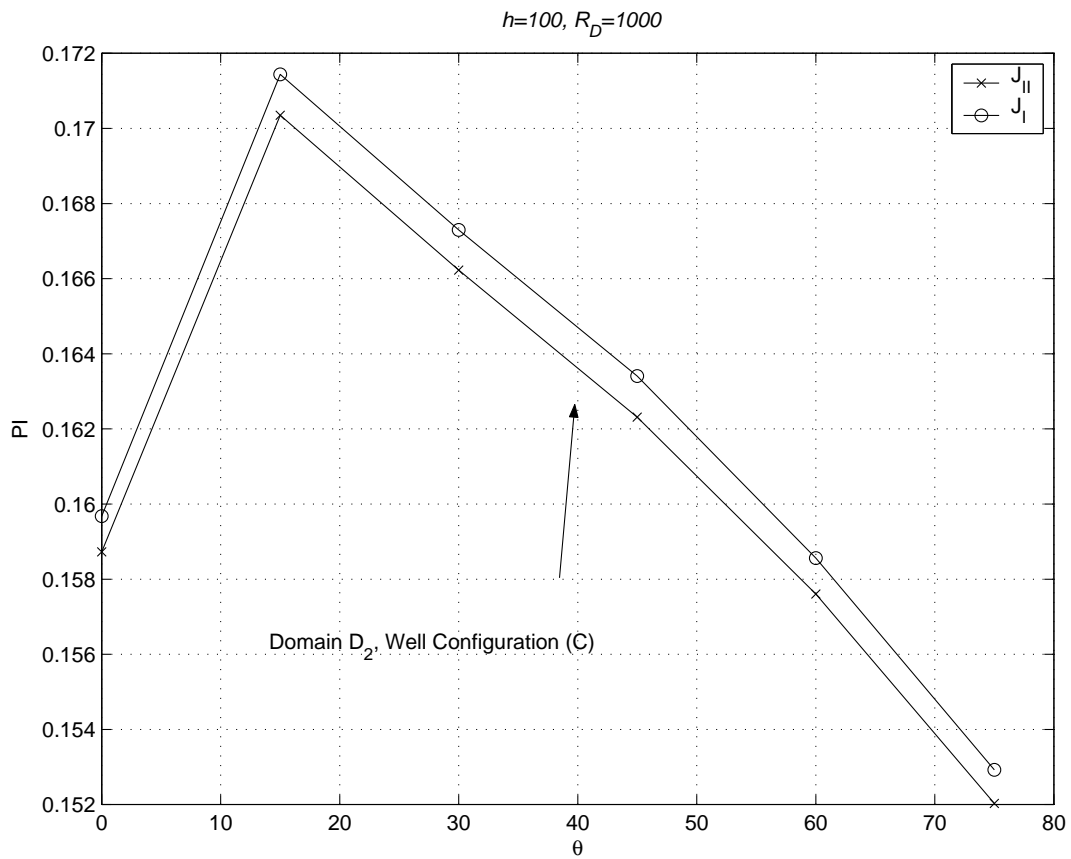


Fig. 22. Productivity Indices for Domain D_2 , Well Configuration (C).

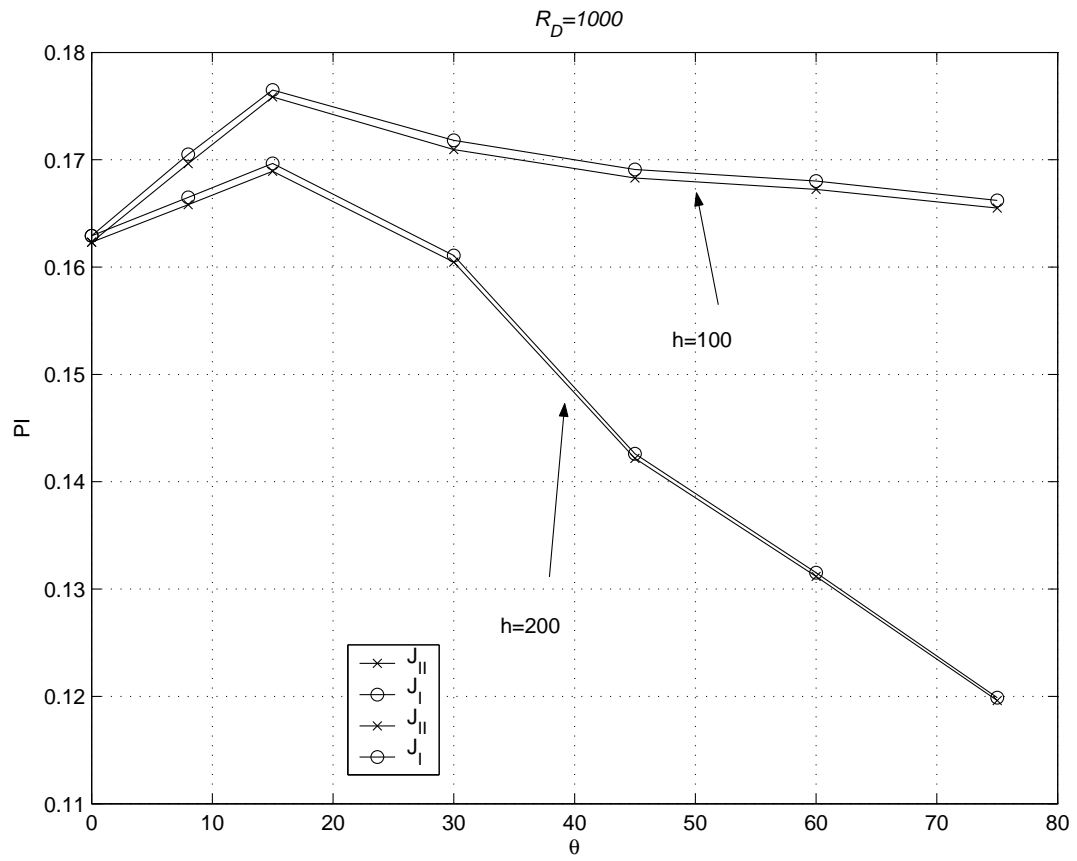


Fig. 23. Productivity Indices for Domain D_1 , Well Configuration (C).

Table 10.: Productivity Indices for Domain D_1 , Well Configuration (C).

	θ	0	8	15	30	45	60	75
$h = 100$	J_I	0.1629	0.1705	0.1765	0.1718	0.1691	0.1680	0.1662
	J_{II}	0.1623	0.1696	0.1758	0.1710	0.1683	0.1672	0.1655
	$\frac{J_I - J_{II}}{J_{II}}$, percent	0.36	0.50	0.37	0.50	0.48	0.46	0.47
$h = 200$	J_I	0.1629	0.1665	0.1697	0.1611	0.1426	0.1315	0.1199
	J_{II}	0.1623	0.1658	0.1689	0.1605	0.1422	0.1312	0.1196
	$\frac{J_I - J_{II}}{J_{II}}$, percent	0.36	0.41	0.43	0.38	0.30	0.27	0.28

B. Horizontal Well

Due to large size of the reservoir, the pseudo-steady-state and boundary-dominated indices do not differ significantly from each other for the considered three dimensional domains and well configurations, as shown in the previous section. Therefore, the numerical study for horizontal wells was restricted to the cylindrical domain D_1 .

Methods presented in [22, 15] rely heavily on the assumption that the vertical dimension of the reservoir is small compared to the penetration length of the well. Moreover, as noted in [22], the precision of the evaluation of the productivity index for horizontal wells decreases drastically as the distance from the well to vertical boundaries of the reservoir becomes comparable to the distance to the top and/or the bottom of the reservoir, if the reduction to the two-dimensional problem is used. This section presents computational results for such settings when the assumption of

the small reservoir thickness and the well being clearly inside the drainage area are relaxed.

Consider a horizontal well of length L modeled by configuration (D), i. e. the well is located at equal distances from the top and the bottom of the reservoir. The thickness of the reservoir is fixed at $h = 100$ for all penetration lengths. As seen from Table 11 and Fig.24, the difference between the pseudo-steady-state and boundary-dominated productivity indices is significant for long horizontal wells.

An interesting question is when the effects of the flow in the vertical direction from the top and the bottom of the reservoir become too significant to approximate by a geometrical skin factor s_g . For that purpose the productivity indices J_I and J_{II} were computed for the well configuration (D) with penetration length $L = 1500$ for various values of the reservoir thickness h . The results are presented in Table 12.

Table 11.: Productivity Indices for Domain D_1 , Well Configuration (D), Various Values of L .

L	500	700	900	1100	1300	1500
J_I	0.5190	0.6750	0.8521	1.0399	1.2299	1.4147
J_{II}	0.5038	0.6475	0.8069	0.9707	1.1281	1.2677
$\frac{J_I - J_{II}}{J_{II}}$, percent	3.02	4.25	5.60	7.13	9.03	11.59

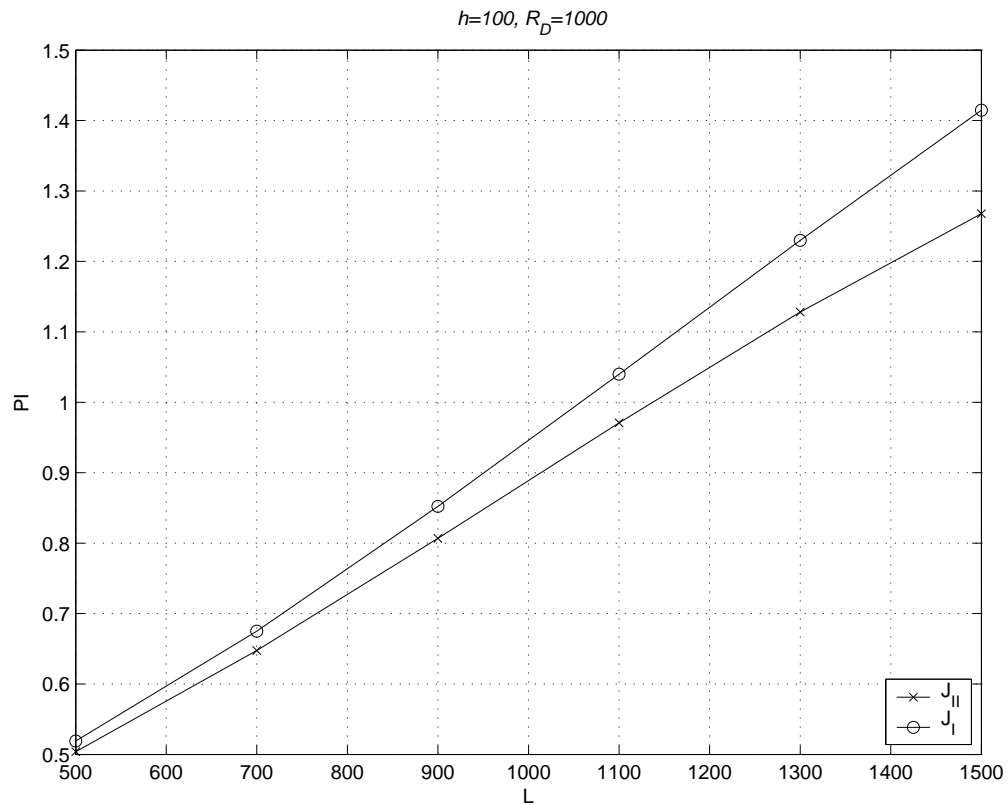


Fig. 24. Productivity Indices for Domain D_1 , Well Configuration (D).

Table 12.: Productivity Indices for Domain D_1 , Well Configuration (D), Various Values of h .

h	100	200	300	400	500
J_I	1.4147	1.0286	0.7887	0.6303	0.5156
J_{II}	1.2677	0.9703	0.7625	0.6171	0.4973
$\frac{J_I - J_{II}}{J_{II}}$, percent	11.59	6.01	3.44	2.14	3.68

The last setting considered is a horizontal well with configuration (E), located at distance d below the plane of symmetry of domain D_1 . The graphs of the computed

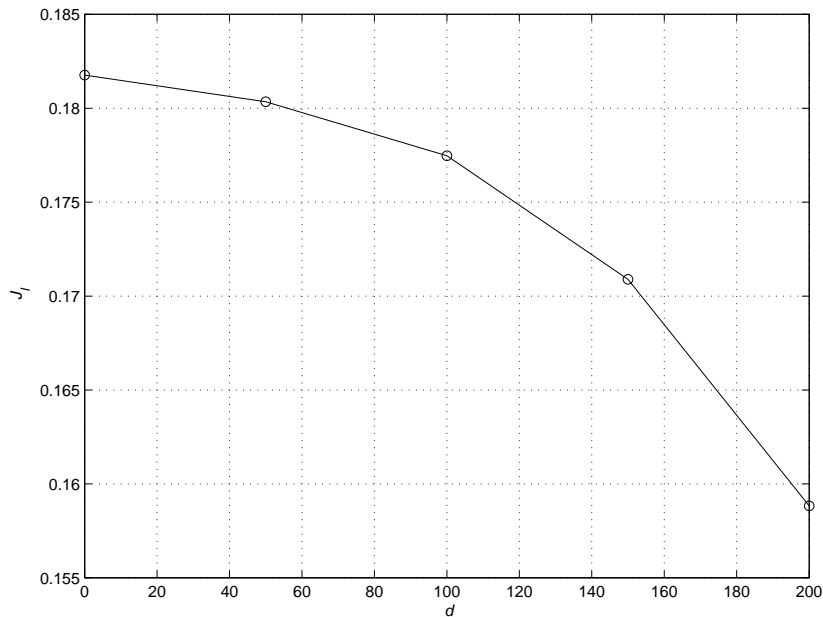


Fig. 25. Pseudo-steady-state Productivity Index for Various Values of d , Well Configuration (E), $h = 500$, $L = 500$.

pseudo steady state productivity index J_I as a function of distance d from the center of the reservoir for various penetration lengths L are shown in Figs.25-31.

For all practical purposes, one can conclude that the optimal location of a horizontal well in a cylindrical reservoir D_1 is in the horizontal plane of symmetry of the reservoir. Note that for long wells, however, the pseudo steady state productivity index slightly increases for small values of d . This may be an indication of interesting feature of the diffusive capacity as a geometrical characteristic defined through the first eigenvalue λ_0 . The latter is sensitive to the location of the well relative to the planes and lines of symmetry of the domain, as it is comprehensively illustrated in the section Productivity Index in a Two-dimensional Reservoir. In three dimensional domains, there are more such planes and lines of symmetry and, therefore, there may be several well configurations yielding maximal productivity index.

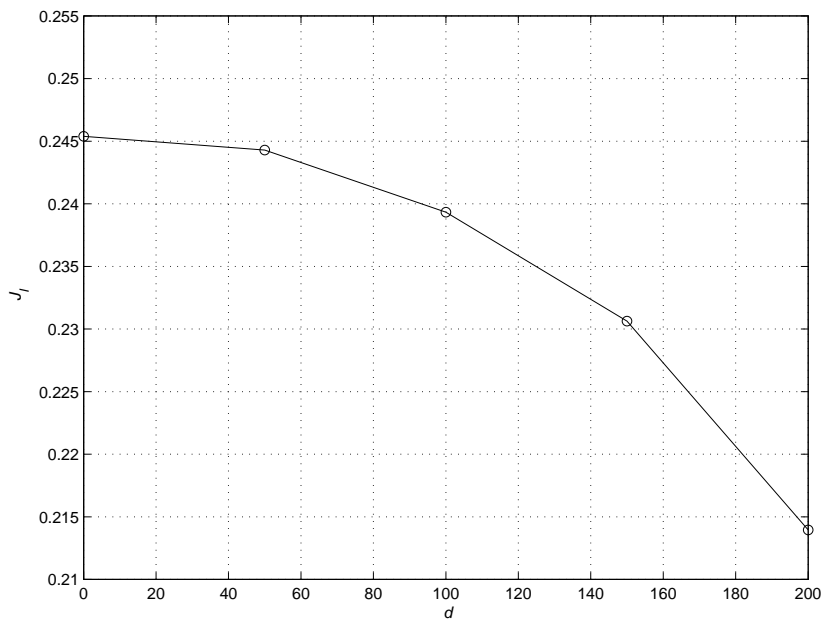


Fig. 26. Pseudo-steady-state Productivity Index for Various Values of d , Well Configuration (E), $h = 500$, $L = 700$.

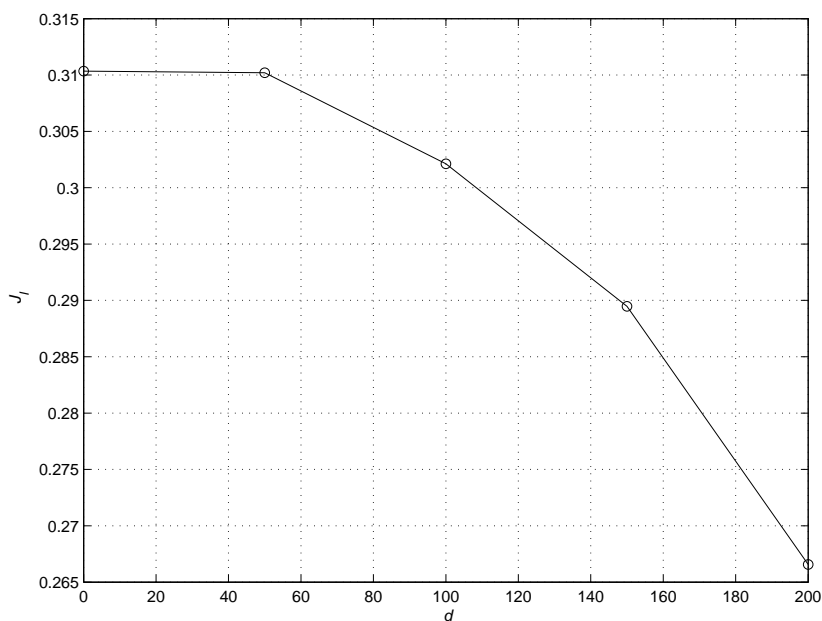


Fig. 27. Pseudo-steady-state Productivity Index for Various Values of d , Well Configuration (E), $h = 500$, $L = 900$.

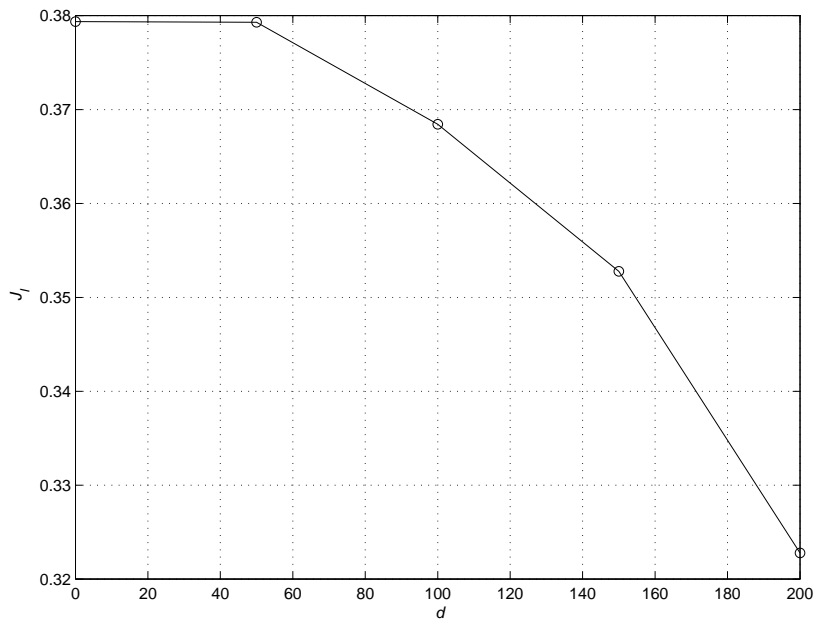


Fig. 28. Pseudo-steady-state Productivity Index for Various Values of d , Well Configuration (E), $h = 500$, $L = 1100$.

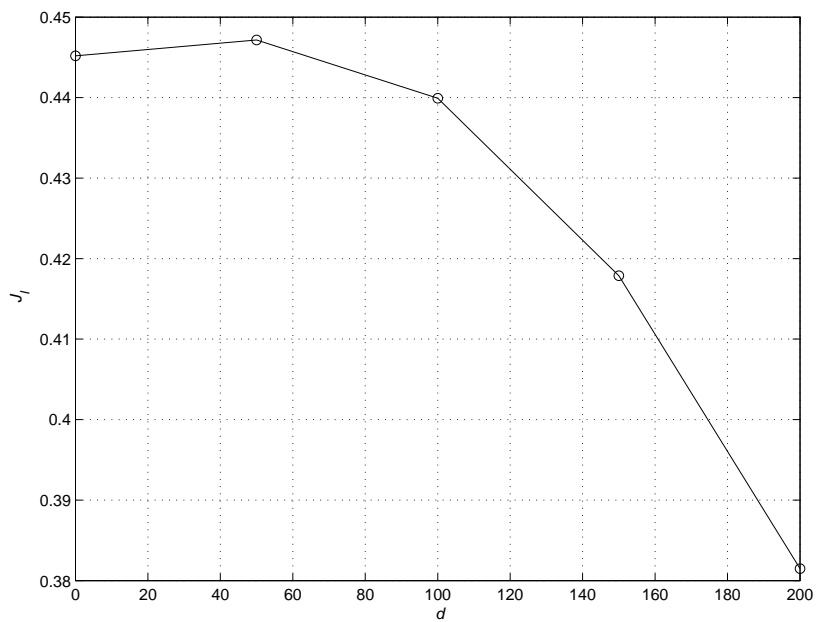


Fig. 29. Pseudo-steady-state Productivity Index for Various Values of d , Well Configuration (E), $h = 500$, $L = 1300$.

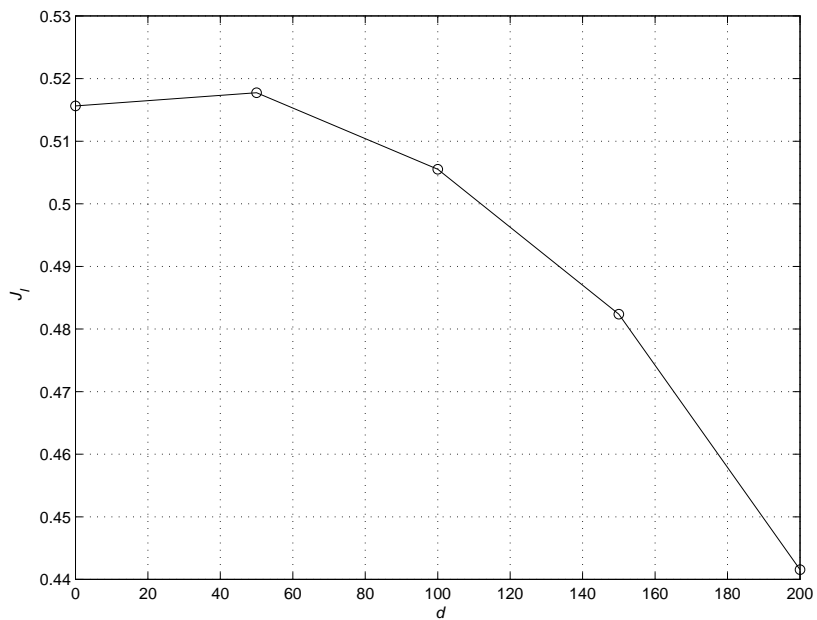


Fig. 30. Pseudo-steady-state Productivity Index for Various Values of d , Well Configuration (E), $h = 500$, $L = 1500$.

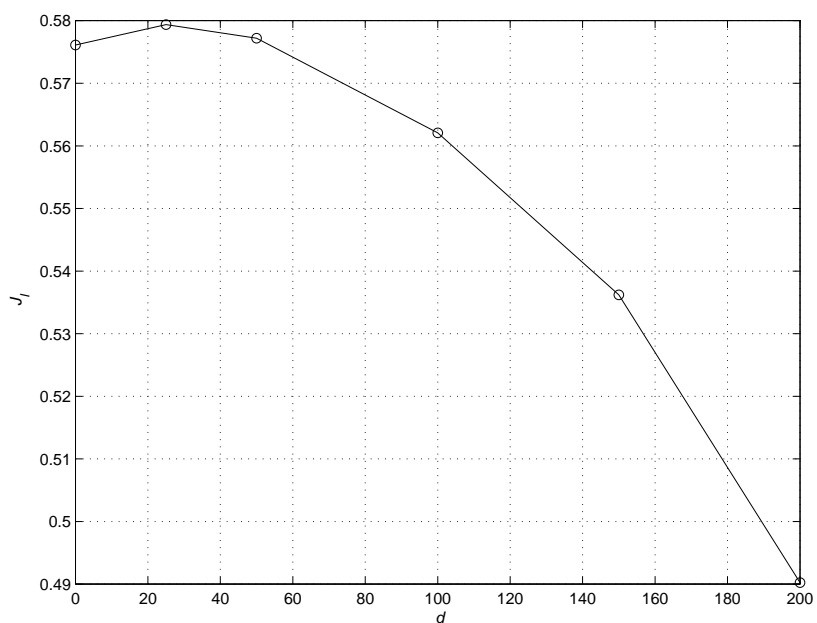


Fig. 31. Pseudo-steady-state Productivity Index for Various Values of d , Well Configuration (E), $h = 500$, $L = 1700$.

CHAPTER IX

REMARKS ON NUMERICAL CALCULATIONS

A. Computations in Two-dimensional Domains

The corresponding boundary value and eigenvalue problems were solved by the finite element method, implemented in the MatLab Partial Differential Equations Toolbox. The following is the command line Matlab code used for evaluation of the diffusive capacities J_I and J_{II} in a domain shown in Fig.10 for orthotropic media with $k_y/k_x = k$ (see section Orthotropic Media).

```
% The following function computes the BD and PSS PI's for the problem
% with the orthotropic media, where:
% A (the coefficient matrix) =[c11, 0]
%                               [0, c22] and c22:c11=kk:1;
% INPUT Parameters: kk
% OUTPUT Parameters: see below

function [JJ] = PI(kk);

n=6;

% JJ - the output array is defined as follows:
% [k,m,n]=size(JJ), where m is 4 and n is the size or the array of
% r's (the dimensionless radius);
% k is 2 - analyzing two shapes (for two different curvature
```

```
% exponents alpha)
% JJ(1) - first row is reserved for boundary dominated PI of the
% shape
% JJ(2) - second row is reserved for PSS PI of the shape
% JJ(3) - third row is the relative difference
% JJ(4) - first eigenvalues of the elliptic problem

JJ=zeros(2,4,n);

%initialize r's
%rr- dimensionless radius of the circle with the same area

rr=zeros(1,n);
rr(1)=10.;
rr(2)=50.;
rr(3)=100.;
rr(4)=500;
rr(5)=1000;
rr(6)=10000;

for i=6:6

% initialize alpha - the exponent of "curvature"

alph(1)=0.2;
alph(2)=0.4;
```

```
alph(3)=0.6;
alph(4)=0.8;
alph(5)=1;

%r=radius of the ascribed circle

r=2*rr(i)/sqrt(3)*sqrt(pi/sqrt(3));

ya = 0.;
xb = 0.;
yb = 0.;
xc = 0.;

for ia=3:4

% set up the parameters of the geometry

if ia==3                                % alpha= 0.6
    xa = 12533.14137;
    yc=66843.42064;
    k=66843.42064;
    xW = 3856.351191;
    yW = 18230.02381;
end;

if ia==4                                % alpha= 0.8
```

```
    xa = 12533.14137;
    yc=56399.13616;
    k=56399.13616;
    xW = 4028.509725;
    yW = 17353.58036;
end;

%STEP 1. Specifying curvilinear outer triangle geometry

%side 1 - straight

k1=(yb-ya)/(xb-xa);
b1=yb-xb*k1;

nth=40;
th=linspace(xa,xb-(xb-xa)/nth,nth);
xt=th;
yt=k1*th+b1;
p1=[xt; yt];

%side 2 - straight
th=linspace(yb,yc-(yc-yb)/nth,nth);
yt=th;
xt=0.*yt;
p2=[xt; yt];
```

```

%side 3 - curvilinear
th=linspace(xc,xa-(xa-xc)/nth,nth);
xt=th;
xnth=size(xt,2);
yt=zeros(1,xnth);
for it=1:xnth
    yt(it)=k*(1.-(xt(it)/xa)^alph(ia));
end;
p3=[xt; yt];
p1=[p1 p2 p3]';
p1n=size(p1,1);

dl1=[2*ones(1,p1n); p1(:,1)'
     p1(2:p1n,1)' p1(1,1)'
     p1(:,2)'
     p1(2:p1n,2)' p1(1,2)'
     zeros(1,p1n);
     ones(1,p1n);
     zeros(1,p1n) ;
     zeros(1,p1n) ;
     zeros(1,p1n)];

% inner circle

gd1=zeros(4,1);
gd1(1,1)=1;

```

```

gd1(2,1)=xW;
gd1(3,1)=yW;
gd1(4,1)=1;
dl4=decsg(gd1);
dl4n=size(dl4,2);

% create the Geometry matrix

for it=1:dl4n
    dl4(6,it)=0;
    dl4(7,it)=1;
end; %for it

dl=[dl1,dl4];

%STEP 2. Specify boundary conditions

% create boundary conditions matrix

    [dlm dln]=size(dl);
    dl1n=size(dl1,2);
    b1=zeros(10,dln);
    for ll=1:dln

% if the edge is on the inner circle of the well then- Dirichlet
% condition

```



```
if ll>d11n

    b1(1,ll)=1;
    b1(2,ll)=1;
    b1(3,ll)=1;
    b1(4,ll)=1;
    b1(5,ll)=1;
    b1(6,ll)=1;
    b1(7,ll)='0';
    b1(8,ll)='0';
    b1(9,ll)='1';
    b1(10,ll)='0';

end;

% if the piece is on the outer boundary then- Neumann
% condition

if ll<=d11n

    b1(1,ll)=1;
    b1(2,ll)=0;
    b1(3,ll)=1;
    b1(4,ll)=1;
    b1(5,ll)='0';
    b1(6,ll)='0';
    b1(7,ll)='0';
    b1(8,ll)='0';
```

```
                b1(9,11)='1';
                b1(10,11)='0';
            end;
        end; %for ll

% create mesh

        [p,e,t]=initmesh(dl);
        [p,e,t]=refinemesh(dl,p,e,t);
        [p,e,t]=refinemesh(dl,p,e,t);
        p=jigglemesh(p,e,t);

% initialize the coefficient matrix

        cc=zeros(2,1);
        cc(1,1)=1;
        cc(2,1)=kk;

% Solve the Poisson's problem

        u=asempde(b1,p,e,t,cc,0,-2./(rr(i)^2-1.));

%compute J_I

        [ar,a1,a2,a3]=pdetrp(p,t);
        ut=pdeintrp(p,t,u);
```

```

[m,nn]=size(ut);
vol=0.;
ss=0.;

for ii=1:nn
    vol=vol+ar(ii);
    ss=ss+ut(ii)*ar(ii);
end;% ii

uhat=ss/vol;
[m,n1]=size(e);
k=0;
s=0;

for ii=1:n1
    if ((p(1,e(1,ii))-xW)^2+(p(2,e(1,ii))-yW)^2)<1.01)
        k=k+1;
        s=s+u(e(1,ii));
    end;
end;% ii

uhat1=s/k

JJ(ia-2,2,i)=1/(uhat1-uhat);

% Compute the eigenvalues of the elliptic problem:
% a) determine the range of search of the eigenvalues

```

```

% (empirically found)

    if i==5
        max=0.00001
    end; %if

    if i==6
        max=1.e-07
    end; %if

% b) compute the eigenvalues and eigenfunction
    [v,l]=pdeeig(b1,p,e,t,cc,0,1,[0 max]);

% save the lambda

    JJ(ia-2,4,i)=l(1);

% compute and save the BD PI

    JJ(ia-2,1,i)=l(1)*(rr(i)^2-1)/2;

    JJ(ia-2,3,i)=abs((JJ(ia-2,1,i)-JJ(ia-2,2,i))/JJ(ia-2,2,i));
end; %for ia

end; %for i

```

For various values of kk , function PI is called from the main procedure, which saves the output results into a file.

```
res=zeros(2,9,4,6);
kk=zeros(1,9);
kk(1)=1;
kk(2)=10;
kk(3)=20;
kk(4)=50;
kk(5)=100;
kk(6)=1./10;
kk(7)=1./20;
kk(8)=1./50;
kk(9)=1./100;

savefile=('CurvTri_Anistropy10000.mat');

for ia=1:2
for ii=1:9
    res1= PI(kk(ii));
    for k=1:4
        for ll=1:6
            res(ia,ii,k,ll)=res1(ia,k,ll)
        end; %ll
    end; %kk
```

```

end; %ii
end; %ia

save(savefile,'res');

```

The use of Matlab PDE toolbox restricts the freedom to manage the parameters of the numerical computations, in particular, the parameters of the discretization of a domain. Since the shape of a domain is crucial to the difference of the two productivity indices, it is important to establish the precision of the computational results.

To examine the computational results, consider a particular case - domain depicted on the Fig.10 of chapter Productivity Index in a Two-dimensional Reservoir. Here, the curvilinear edge of the domain is described by the equation $y = b \left(1 - \left(\frac{x}{a}\right)^{0.2}\right)$. The area of the domain is $\pi 1.0E6$. Of all considered two-dimensional domains, this shape has the most complex geometry for finite element discretization.

The quality of each finite element in the initial triangulation produced by PDE Toolbox is measured by the formula

$$q = \frac{4\sqrt{3a}}{(h_1^2 + h_2^2 + h_3^2)^{1/2}}, \quad (9.1)$$

where a is the area and h_1 , h_2 and h_3 the side lengths of the triangle. If $q > 0.6$ the triangle is of acceptable quality (aspect ratio) [23]. For the triangulation of the domain being analyzed, less than 8% of the triangles are of the bad quality ($q < 0.6$) and the average value of q for the "bad" triangles is 0.36.

Table 13 provides the evidence that the computations of the J_{PSS} for this particular domain are stable. J_{PSS} is computed for 5 consecutively refined grids. Each time

the grid refinement is achieved by dividing each triangular element into four similar ones. Note that the quality of the triangulization does not change with refinement.

Table 13.: Effect of Grid Refinement on Computations of J_{PSS} .

Order of refinement	J_{PSS}
0	0.0864
1	0.0860
2	0.0859
3	0.0859
4	0.0859

Table 14 lists the values of J_{BD} and λ_0 computed for the same as in Table 13 5 consequently refined grids.

Table 14.: Effect of Grid Refinement on Computations of J_{BD} and λ_0 .

Order of refinement	λ_0	J_{BD}
0	0.6607E-07	0.0330
1	0.6604E-07	0.0330
2	0.6603E-07	0.0330
3	0.6603E-07	0.0330
4	0.6603E-07	0.0330

The obtained results enable us to estimate the order of the error of computations. The method is based on the following observation [2]. Let λ is the true first eigenvalue

of the problem (here the subscript 0 is omitted for convenience) and λ_h is the numerical approximation of the first eigenvalue on the grid of diameter h . Suppose, the error of computations is of order α , i. e.

$$|\lambda - \lambda_h| \leq Ch^\alpha, \quad (9.2)$$

where C is a constant. For the next regular grid refinement, the diameter of the grid reduces by factor 2. Using the approximations of the first eigenvalue from several consecutively refined grids and the equation (9.2), the following formula can be used for estimation of the order of approximation α :

$$\frac{|\lambda_h - \lambda_{h/2}|}{|\lambda_{h/2} - \lambda_{h/4}|} \leq 2^\alpha. \quad (9.3)$$

Let λ_i be the first eigenvalue computed on the grid refined i times. The difference $\lambda_3 - \lambda_4$ is negligibly small, therefore, the last two approximations are excluded, however, the approximations of orders 0 to 3 give the results summarized in Table 15.

Table 15.: Order of Approximation of λ_0 .

$\frac{ \lambda_0 - \lambda_1 }{ \lambda_1 - \lambda_2 }$	4.01
$\frac{ \lambda_1 - \lambda_2 }{ \lambda_2 - \lambda_3 }$	4.01

Thus, $\alpha = 2$, implying

$$|\lambda - \lambda_h| \leq Ch^2, \quad (9.4)$$

B. Computations in Three-dimensional Domains

All numerical experiments presented in the section Productivity Index in a Three-dimensional Reservoir were implemented in the software package FEMLAB, which utilizes finite element and finite volume methods for solving boundary value problems,

both steady state and transient, in one, two and three dimensions. Boundary value problem (4.3)-(4.5) and the eigenvalue problem (4.24)-(4.26) were solved by using the Graphical User Interface (GUI) of FEMLAB, therefore no code was created.

The FEMLAB GUI is very convenient for setting the parameters of the computations, such as the desired tolerance level of iterative methods used for solving the systems of linear algebraic equations, the type of preconditioner used, the tolerance level for the iterative method used for approximating the first eigenvalue, etc. However, difficulties were encountered when solving boundary value problems in three dimensional domains. These problems are mostly due to geometrical features of the problem increasing the complexity of the discretization.

The finite volume discretization algorithm, automatically implemented in FEMLAB, is designed to create a mesh consisting of similar tetrahedrons, each of which is intended to have an acceptable quality [11]. For a three dimensional finite element, a measure of quality is computed similarly to a two dimensional one. When a three dimensional solid domain is discretized, a small aspect ratio of horizontal and vertical dimensions of the domain leads to a very fine mesh. There are several solutions to this problem, one of which is scaling the coefficients of the equation in the boundary value problem. For the purpose of practical application, the domains considered for numerical study, had two parameters that could not be changed - the radius of the well $r_w = 1$ and the diameter of the outer boundary $2R_D = 2000$. The well is represented by a perfectly circular cylinder. Scaling the coefficients of the equation corresponds to distortion of the cylindrical well boundary (the cross-section of the well cylinder is an ellipse rather than a circle), leading to erroneous results and conclusions. The automatically generated mesh was very fine. Due to limited machine resources, it made impossible the analysis of the approximation precision by the mesh refinement method used for the two-dimensional calculations. Therefore, to ensure the precision

of the numerical approximation, in each of the cases considered in the section Productivity Index in a Three-dimensional Reservoir, the corresponding problems were solved on two meshes with different parameters, none of which was a refinement of the other. The values of J_I and J_{II} computed on two different meshes differed by less than $1.0\text{E-}03$, i. e. less than by 1%.

CHAPTER X

CONCLUSIONS AND FUTURE DIRECTIONS

The traditional methods of evaluating the productivity index of a well focus on direct solution of the transient problems of fluid flow in porous media. This dissertation presents methods, based on modeling the productivity index by diffusive capacity, that allow one to reduce the evaluation of the productivity index of a well to solution of a stationary problem.

For problem I that models the production regime with a constant production rate, due to non-uniqueness of the solution additional restrictions must be put on the pressure distribution. Two classes of solutions to problem I were considered - a class of solutions corresponding to the pressure distribution which is constant on the wellbore at each moment of time and a class of solutions corresponding to the pressure distribution which has a constant flux on the wellbore. The first class corresponds to the assumption of infinite conductivity of the wellbore. This class is shown to be a stable class of solutions of problem I. For each class, the diffusive capacity is shown to stabilize to a constant value in a long time asymptote. However, the stabilized values of the diffusive capacity are, in general, different for these two classes. This leads to a problem of determining all classes of solutions to problem I, on which the diffusive capacity stabilizes to a constant value and determining this constant value through the solution of a related steady state problem. Such formulation naturally extends to a problem of determining the class of solutions to problem I on which the diffusive capacity attains the maximum value. For instance, long vertical and slanted wells can be modeled by considering gravity effects on the well bore pressure. Such kind of model leads to restricting the solutions of problem I to a certain class of functions.

In the presented numerical results, only such solutions to problem I were consid-

ered that are uniformly distributed on the wellbore. Then the pseudo-steady-state productivity index has a unique constant value defined through a solution of a related steady state problem with a homogeneous Dirichlet condition on the wellbore boundary.

For each of the initial boundary value problems II and III, modeling constant pressure production regime for an ideal well and a well with the skin zone, respectively, the diffusive capacity is proven to be equivalent to the diffusive capacity defined on the solutions of the corresponding Sturm-Liouville problems. In the constant wellbore pressure production regime, the productivity index of a well with zero skin is shown to stabilize to a unique constant value regardless of the initial pressure distribution.

For initial boundary value problem II, the diffusive capacity is determined by geometrical characteristics of the reservoir/well system as reflected in the first eigenvalue λ_0 of the corresponding elliptic operator and the Lebesgue measure of the domain. Using this representation, a well-known variational principle for the first eigenvalue λ_0 implies that the boundary dominated index can be estimated from above and below by the pseudo steady state index through an inequality of the type $J_{II} \leq J_I \leq C_\Omega J_{II}$. The constant C_Ω is fully determined by λ_0 and the normalized eigenfunction ϕ_0 corresponding to λ_0 .

The last observation gives a means to determine when the two characteristics of the well capacity are not equivalent to each other even for practical purposes. The numerical study presented in this dissertation illustrates how an isoperimetric inequality may be used to quantify when the geometry of the reservoir/well system leads to a significant difference between the pseudo-steady-state and boundary-dominated indices. The magnitude of this difference reflects the symmetry of the reservoir/well system, since the first eigenvalue λ_0 is sensitive to the location of the well relative to the lines and center of symmetry of the domain.

The analytical representation of the productivity indices through the solutions of the auxiliary stationary problems, in principle, allows one to include the anisotropy of the porous media in the reservoir. The effect on the behavior of the productivity indices of a type of such anisotropy, orthotropy, was analyzed for two dimensional reservoir/well systems.

The third type boundary condition proves to be an appropriate model of the thin skin effect for damaged wells produced with the constant well bore pressure in a cylindrical reservoir. At the same time, the physical considerations dictate that the third type boundary condition cannot serve as a model of a stimulated well.

One of the advantages of the presented method of evaluation of well productivity is the fact that the boundary value problems to be solved are stationary, which greatly reduces the required computing resources. Using this attractive feature, a numerical study was performed for a general homogeneous three-dimensional reservoir for a variety of well configurations. Several effects were revealed in this study, which pertain to the three-dimensional nature of the fluid flow in the reservoir. For instance, such an effect is the flow in the vertical direction toward a deviated well, which shows that the optimal direction of a deviated well of a fixed length is not always vertical. In a three-dimensional domain, there may be a number of planes and lines of symmetry. Therefore, the problem of optimal location and direction of the well with respect to those becomes more complex than for a two-dimensional domain. One of the numerical experiments described in the last part of the dissertation, showed that the location of the horizontal well yielding the greatest well productivity is not necessarily in the plane of symmetry of the domain. An interesting problem is to investigate the conditions for the optimal (from the point of view of productivity) placement and direction of the well in a three-dimensional reservoir.

REFERENCES

- [1] R. A. Adams, *Sobolev Spaces*, Academic Press, New York, 1975.
- [2] D. Braess, *Finite Elements: Theory, Fast Solvers, and Applications in Solid Mechanics*, 2nd ed., Cambridge University Press, Cambridge, UK, 2001.
- [3] H. Cinco-Ley, H. J. Ramey, Jr., F. G. Miller, *Pseudo-skin factors for partially penetrating directionally drilled wells*, paper SPE 5589, presented at 50th Annual Fall Meeting, Dallas, Texas, September 28–October 1, 1975.
- [4] H. Cinco, F. G. Miller, H. J. Ramey, Jr., *Unsteady-state pressure distribution created by a directionally drilled well*, JPT, Vol. 27, No. 11, (1975), pp. 1392–1400.
- [5] R. Courant, D. Hilbert, *Methods of Mathematical Physics*, Interscience Publisher, Vol. 1, New York, 1953.
- [6] D. N. Dake, *The Practice of Reservoir Engineering*, Elsevier, Amsterdam, 1978.
- [7] D. N. Dietz, *Determination of average reservoir pressure from build-up surveys*, JPT, Vol. 17, No. 4, (1965), pp. 955–959.
- [8] R. C. Earlougher, Jr., *Advances in Well Test Analysis*, SPE of AIME, Dallas, Texas (1977).
- [9] R. C. Earlougher, Jr., H. J. Ramey, Jr., F. G. Miller, Mueller, *Pressure distributions in rectangular reservoirs*, JPT, Vol. 20, No. 2, (1968), pp. 200–208.
- [10] C. L. Evans, *Partial Differential Equations.*, AMS, Providence, Rhode Island, 1998.

- [11] *FEMLAB online support knowledge base*
URL: <http://www.comsol.com/support/knowledgebase>.
- [12] M. J. Fetkovich, *The isochronal testing of oil wells*, paper SPE 4529, presented at 48th Annual Fall Meeting, Las Vegas, Nevada, September 30–October 3, 1973.
- [13] M. J. Fetkovich, E. J. Fetkovich, M. D. Fetkovich, *Useful concepts for decline - curve forecasting, reserve estimation and analysis*, SPE Reservoir Engineering, Vol. 11, No. 1, (1996), pp. 13–22.
- [14] A. Friedman, *Partial Differential Equations of Parabolic Type*, Prentice Hall, New Jersey, 1964.
- [15] P. A. Goode, F. J. Kuchuk, *Inflow performance of horizontal wells*, SPE Reservoir Engineering, Vol. 6, No. 3 (1991), pp. 319–323.
- [16] M. F. Hawkins, Jr., *A note on the skin effect*, Petr. Trans. AIME, 207, (1956), pp. 356–357.
- [17] W. Helmy, and R. A. Wattenbarger, *New shape factors for wells produced at constant pressure*, paper SPE 39970, presented at SPE Gas Technology Symposium, Calgary, Canada, March 15–18, 1998
- [18] W. Hurst, *Establishment of skin effect and its impediment to fluid flow into a well bore*, Petroleum Engineer, 25, (1953), pp. B-6 – B-16.
- [19] W. Hurst, J. D. Clark, E. B. Brauer, *The skin effect in producing wells*, JPT, Vol. 21, No. 11 (1969), pp. 1483–1489.
- [20] A. Ibragimov, P. Valko, *On productivity index in pseudo-steady and boundary dominated flow regimes*, technical report, Institute of Scientific Computations, 2000, <http://www.isc.tamu.edu/iscreports.html>.

- [21] R. F. Krueger, *An overview of formation damage and well productivity in oilfield operations*, JPT, Vol. 38, No. 2, (1986), pp. 131–152.
- [22] L. Larsen, *General productivity models for wells in homogeneous and layered reservoirs*, paper SPE 71613, presented at 2001 SPE Annual Conference and Exhibition, New Orleans, Louisiana, September 30–October 3, 2001.
- [23] *The MathWorks online documentation: Release 13*.
URL:[http : / / www. mathworks. com/ access/ helpdesk/ help/ helpdesk. shtml](http://www.mathworks.com/access/helpdesk/help/helpdesk.shtml)
- [24] C. S. Matthews, F. Brons, and P. Hazebroek, *A method for determination of average pressure in a bounded reservoir*, Trans. AIME, 201, (1954), pp. 182–191.
- [25] V. G. Maz'ya, *Differentiable Functions on Bad Domains*, World Scientific, Singapore, 1997.
- [26] S. G. Mikhlin, *Linear Equations of Mathematical Physics*, Holt, Rinehart and Winston, Inc., New York, 1967.
- [27] M. Muskat, *The Flow of Homogeneous Fluid Through Porous Media*, McGraw-Hill, New York, 1937.
- [28] J. K. Pucknell, P. J. Clifford, *Calculations of total skin factors*, paper SPE 23100, presented at Offshore Europe Conference, Aberdeen, UK, September 3–6, 1991.
- [29] R. Raghavan, *Well Test Analysis*, Prentice Hall, New York, 1991
- [30] H. J. Ramey, Jr., W. M. Cobb, *A general pressure buildup theory for a well in a closed drainage area*, JPT, Vol. 23, No. 12 (1971), pp. 1493–1505.

- [31] C. V. Theis, *The relationship between the lowering of the piezometric surface and the rate and duration of discharge using ground water storage*, Trans. AGU, Vol. 16, (1935), pp. 519–524.
- [32] L. C. Uren, *Petroleum Production Engineering*, McGraw-Hill, New York, 1946.
- [33] A. F. van Everdingen, and W. Hurst, *The application of the laplace transformation to flow problems in reservoirs*, Trans. AIME, 186, (1949), pp. 305–324.
- [34] A. F. van Everdingen, *The skin effect and its influence on the productivity capacity of a well*, Petroleum Trans. AIME, 198, (1953), pp. 171–176.
- [35] T. Yildiz, *Assessment of total skin factors in perforated wells*, paper SPE 82249, presented at SPE European Formation Damage Conference, Hague, Netherlands, May 13–14, 2003.

VITA

Dinara Khalmanova

PERMANENT ADDRESS:

Pereulok Utrennii, 5
Karaganda, 470038,
Kazakhstan, CIS

CURRENT ADDRESS:

700, Dominik Dr, Apt 508,
College Station, TX, 77840
(979)-695-8104
dkhalmanova@lycos.com

Education:

M.S. Texas A&M University, Mathematics, May, 1999.

B.S. Karaganda State University, Kazakhstan, Mathematics, June 1997.

Research Interests:

applied mathematics, Mathematical modeling, biomathematics, flow in porous media.

The typist for this thesis was Dinara Khalmanova.